



Review

# PCD Genes—From Patients to Model Organisms and Back to Humans

Michał Niziołek <sup>1</sup>, Marta Bicka <sup>1,2</sup>, Anna Osinka <sup>1</sup>, Zuzanna Samsel <sup>1</sup>, Justyna Sekretarska <sup>1</sup>, Martyna Poprzeczko <sup>1,3</sup>, Rafał Bazański <sup>1</sup>, Hanna Fabczak <sup>1</sup>, Ewa Joachimiak <sup>1,\*</sup> and Dorota Włoga <sup>1,\*</sup>

<sup>1</sup> Laboratory of Cytoskeleton and Cilia Biology, Nencki Institute of Experimental Biology, Polish Academy of Sciences, 3 Pasteur Street, 02-093 Warsaw, Poland; m.niziolek@nencki.edu.pl (M.N.); m.bicka@nencki.edu.pl (M.B.); a.osinka@nencki.edu.pl (A.O.); z.samsel@nencki.edu.pl (Z.S.); j.sekretarska@nencki.edu.pl (J.S.); martyna.poprzeczko@wum.edu.pl (M.P.); raflik@gmail.com (R.B.); h.fabczak@nencki.edu.pl (H.F.)

<sup>2</sup> Faculty of Chemistry, University of Warsaw, 1 Pasteur Street, 02-093 Warsaw, Poland

<sup>3</sup> Laboratory of Immunology, Mossakowski Medical Research Institute, Polish Academy of Sciences, 5 Pawinskiego Street, 02-106 Warsaw, Poland

\* Correspondence: e.joachimiak@nencki.edu.pl (E.J.); d.włoga@nencki.edu.pl (D.W.); Tel.: +48-22-58-92-338 (E.J. & D.W.)

**Abstract:** Primary ciliary dyskinesia (PCD) is a hereditary genetic disorder caused by the lack of motile cilia or the assembly of dysfunctional ones. This rare human disease affects 1 out of 10,000–20,000 individuals and is caused by mutations in at least 50 genes. The past twenty years brought significant progress in the identification of PCD-causative genes and in our understanding of the connections between causative mutations and ciliary defects observed in affected individuals. These scientific advances have been achieved, among others, due to the extensive motile cilia-related research conducted using several model organisms, ranging from protists to mammals. These are unicellular organisms such as the green alga *Chlamydomonas*, the parasitic protist *Trypanosoma*, and free-living ciliates, *Tetrahymena* and *Paramecium*, the invertebrate *Schmidtea*, and vertebrates such as zebrafish, *Xenopus*, and mouse. Establishing such evolutionarily distant experimental models with different levels of cell or body complexity was possible because both basic motile cilia ultrastructure and protein composition are highly conserved throughout evolution. Here, we characterize model organisms commonly used to study PCD-related genes, highlight their pros and cons, and summarize experimental data collected using these models.



**Citation:** Niziołek, M.; Bicka, M.; Osinka, A.; Samsel, Z.; Sekretarska, J.; Poprzeczko, M.; Bazański, R.; Fabczak, H.; Joachimiak, E.; Włoga, D. PCD Genes—From Patients to Model Organisms and Back to Humans. *Int. J. Mol. Sci.* **2022**, *23*, 1749. <https://doi.org/10.3390/ijms23031749>

Academic Editor: Thomas Falguières

Received: 30 December 2021

Accepted: 31 January 2022

Published: 3 February 2022

**Publisher's Note:** MDPI stays neutral with regard to jurisdictional claims in published maps and institutional affiliations.



**Copyright:** © 2022 by the authors. Licensee MDPI, Basel, Switzerland. This article is an open access article distributed under the terms and conditions of the Creative Commons Attribution (CC BY) license (<https://creativecommons.org/licenses/by/4.0/>).

## 1. Introduction—Cilia Diversity

A considerable number of human diseases are caused by genetic mutations that can be passed down from an individual carrying the mutation to the offspring. Ciliopathies are an example of such hereditary genetic disorders with a common feature—the assembly of dysfunctional cilia or their absence.

Cilia, the hair-like cell protrusions play an essential role in human development, body functioning, and reproduction. Based on the ultrastructural organization and functions, cilia can be divided into two main categories: immotile sensory cilia and motile cilia that actively beat. In mammals, sensory cilia are most often formed as a single structure. The most ubiquitous are so-called primary cilia. These a few micrometers long protrusions are formed by the vast majority of non-dividing cells [1,2]. In photoreceptor cells (rods and cones), the sensory cilium is uniquely modified to accommodate a large amount of light-absorbing molecules [3,4]. In the inner ear, an immotile kinocilium assembled by cochlear hair cells is accompanied by numerous highly organized actin-containing mechanosensory

protrusions called stereocilia or stereovilli and plays a role in their proper arrangement [5,6]. In contrast to these monociliated cells, olfactory sensory neurons are multiciliated and form up to 10–30 olfactory cilia (that are usually 50–60  $\mu\text{m}$  long) on the dendritic knob [5,7].

Generally, motile cilia arise as multiple organelles per cell (from several dozen to ~250) [8]. These 5–10  $\mu\text{m}$  long organelles are assembled by epithelial cells lining nasal passages, respiratory tracts [9–11], brain ventricles (in mouse, up to 50 cilia in E1 ependymal cells but one or two cilia in E2 cells (of note, E3 cells assemble single short primary cilium)) [12–15], oviducts [16,17], and efferent ducts connecting testis with epididymis [18–23]. Unusual motile cilia are assembled as monocilia by sperm cells (called flagella) and cells in the embryonic node [24,25]. The sperm's flagella are significantly longer (~60  $\mu\text{m}$ ) than cilia assembled by the epithelial cells and contain additional sperm flagella-specific structures, while nodal cilia lack some of the typical motile cilia components [25–28].

Cilia of all types contain a uniquely organized microtubular scaffold (an axoneme) that originates from the basal body, which serves as the axoneme template and anchors cilium to the cell surface. A short fragment immediately distal to the basal body is called a transition zone and contains peripheral doublets and unique multiprotein complexes (Y-links) but lacks central microtubules (which originate above this region). The transition zone, together with transition fibers, functions as a ciliary gate [29,30].

In most sensory cilia, the axoneme (at least in the proximal part of the cilium) is composed of nine peripherally positioned microtubular doublets ( $9 \times 2 + 0$  organization) that are extensions of two more inner tubules of basal body triplets (a peripheral doublet is composed of a complete 13-protofilament tubule A and 11-protofilament tubule B attached to the wall of tubule A and thus sharing some of tubule A protofilaments; worth mentioning, out of these 11 protofilaments, only 10 are built of tubulin heterodimers). Interestingly, it was recently shown that in primary cilia from MDCK-II cells, the ciliary microtubules are accompanied by actin filaments [31].

Typical motile cilia and sperm flagella, besides peripheral doublets, also have two centrally positioned singlet microtubules ( $9 \times 2 + 2$  organization). Moreover, in typical motile cilia and sperm flagella, both peripheral and central microtubules serve as docking sites for numerous multiprotein complexes, forming a highly organized pattern along the entire cilium length (Figure 1).

Motile cilium cross-section

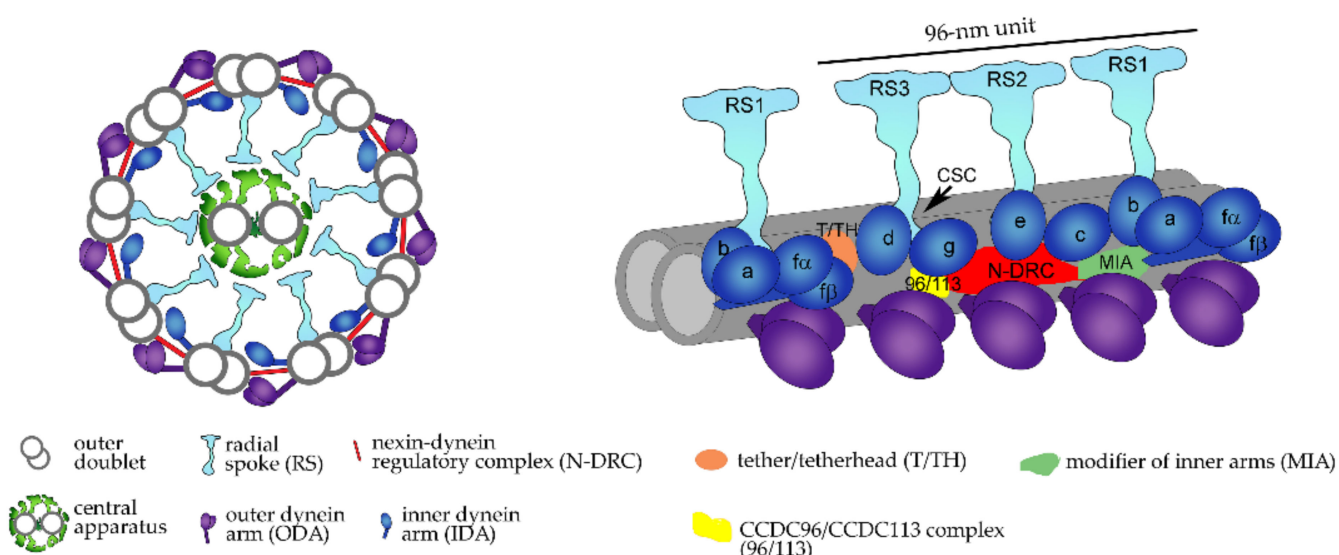


**Figure 1.** Schematic representation of the motile cilium ultrastructure. Cilium cross-section (on the left, view from the side of the basal body) and a 96 nm-long fragment of the outer doublet with docked

ciliary complexes (called the 96 nm axonemal unit, on the right). Each axonemal unit contains four outer dynein arms (ODAs, in violet); seven inner dynein arms: heterodimeric ( $\alpha$ ,  $\beta$ ) IDAf/I1 and single-headed IDA a, b, c, e, g, and d, (dark blue); the nexin-dynein regulatory complex (N-DRC, red) that coordinates the activity of ciliary complexes within the axonemal unit and connects two adjacent outer doublets; and three radial spokes (RS, cyan) that transiently interact with central apparatus projections via their heads, while the base of the stalk comes in contact with two different IDAs [32]. The main complexes are accompanied by several minor complexes that modulate and/or connect large ciliary complexes (e.g., tether/tether head complex (T/TH, orange [33]) positioned near IDA f/I1, CSC complex positioned at the bases of RS2 and RS3 (location indicated by an arrow) [34,35], MIA complex (green) connecting N-DRC and IDA f/I1 [36], and CCDC113/CCDC96 linker (yellow) connecting RS3, N-DRC, and IDAg [37].

Outer and inner dynein arms (ODAs and IDAs), radial spokes (RSs), and nexin links (N-DRCs) are the main complexes attached to peripheral doublets, while projections and a connecting bridge are central microtubule-associated structures [32,38].

In some cell types, along the cilium length, the microtubules' configuration diverges from the most common patterns of organization. Recent studies on primary cilia revealed that  $9 \times 2 + 0$  organization is apparent in the proximal part of the cilia, while in the distal part, microtubules form a bundle of gradually terminating doublets and singlets (A tubules) [31,39]. The number of ciliary microtubules also undergoes a reduction in the distal part of the photoreceptors and olfactory cilia. Photoreceptors can be morphologically and functionally divided into three compartments: (i) the most distal, light-sensitive outer segment, (ii) the organelle-containing (including cilium basal body) inner segment, and (iii) the connecting cilium, enabling transport between the inner and outer segments. In the connecting cilium, microtubules have a  $9 \times 2 + 0$  organization, while in the outer segment, doublets are gradually reduced to singlets, and microtubules dislocate and lose the nine-fold symmetry [4,5]. Similarly, olfactory cilia have the  $9 \times 2 + 2$  configuration in the proximal cilium, but peripheral doublets are reduced to singlets in the distal part (worthy of note is that these cilia are immotile as they lack dynein arms) [5,9]. Ultrastructural studies on mice and guinea pigs showed that the sensory kinocilium in the auditory organ has a  $9 \times 2 + 2$  organization [5,40]. However, some researchers have also observed cilia missing the central apparatus ( $9 \times 2 + 0$ ) [41,42]. Kinocilia have some of the motile cilia multiprotein complexes such as the outer dynein arms and radial spokes but lack the inner dynein arms [6,42].

The sensory cilia function as antennas that receive signals from the surrounding environment and transduce them to the cell body. Although motile cilia can also perform sensory functions [43,44], their primary role is to generate a shift or circulation of the surrounding environment, or to enable cell motility. In humans, the coordinated movement of motile cilia enables the expulsion of the inhaled bacteria and particles, together with the mucus produced by the epithelial cells, out of the respiratory system (mucociliary clearance), generates a circulation of the cerebrospinal fluid through the brain ventricles, supports the transport of the oocyte and early embryo in the Fallopian tube, and likely, as in mouse, the passage of sperm cells through efferent ducts [16,23,45–48]. Long, single flagellum enables sperm cell motility. During embryonic development, the rotatory movement of nodal cilia generates the left-directed nodal flow and consequently plays a role in establishing the left-right asymmetry of the visceral body organs [28,49].

The lack or improper functioning of motile cilia causes reoccurring respiratory infections that lead to bronchiectasis and lung damage; in some affected individuals cilia/flagella dysfunction results also in subfertility or infertility, laterality defects (~50% of affected individuals), and rarely, hydrocephalus [50].

Given the fact that in humans cilia play an important role during embryo development and in physiological processes taking place in already formed tissues and organs, it is not surprising that their dysfunctions cause severe body defects known as ciliopathies. At the base of the etiology of the vast majority of ciliopathies are defects of the primary cilia [51,52], while primary ciliary dyskinesia (PCD) and multiple morphological abnormalities of sperm

(MMAF) are ciliopathies caused by alterations in motile cilia and/or sperm flagella. Similar to other ciliopathies, PCD is a heterogeneous disorder (mostly autosomal recessive) that affects 1 out of 10,000–20,000 individuals [50,53,54]. Up to now, mutations leading to PCD have been detected in nearly 50 genes encoding structural or regulatory proteins that control gene expression, cilia assembly, and functioning [53,55,56]. However, in many cases, the causative mutation(s) remains unknown.

The recent years have brought about significant progress, not only in PCD diagnostics but also in our understanding of the molecular mechanisms behind cilia dysfunction. The advances in our comprehension of the processes regulating cilia formation and motility would not be possible without the extensive cilia-oriented studies conducted in diverse and, compared to humans, simpler model organisms, ranging from protists to mammals. Establishing experimental models with different levels of cell/body complexity was possible because both basic motile cilia ultrastructure and protein composition are highly conserved throughout evolution (it is believed that motile cilia were assembled by the last common ancestor of all current eukaryotes, LECA [57–59]).

More importantly, the genomes of model organisms are fully sequenced, and the methods enabling genome manipulation and the engineering of gene knockouts and knock-ins, mutagenesis, or protein tagging are well-developed. Thus, nowadays, genetic techniques allow researchers to engineer organisms with modifications that correspond to mutations identified in PCD or MMAF-affected individuals and to analyze their outcome at the molecular, ultrastructural, and whole-organism levels. On the other hand, the basic research conducted in model organisms leads to the identification of new ciliary proteins and to the elucidation of their role in ciliogenesis and the regulation of cilia beating. As a result, knowledge regarding ciliary genes, including PCD causative genes, can be transferred in both directions—from patients to model organisms and from model organisms to humans.

Before starting the PCD-related research using model organisms, it is important to ask a simple question: which model will be the most suitable to conduct the planned experiments? In this review, we briefly characterize model organisms commonly used to study the outcome of the mutation(s) in PCD-related genes, highlighting their pros and cons, and then summarize the collected experimental data showing the relationship between gene mutation and its phenotypic outcome in humans and model organisms.

## 2. Single-Celled Models—The Power of Small and Simple

In the case of a multicellular organism, mutations in ciliary genes can affect not only the function of the ciliated cell per se but also the entire development of the organ and/or body as many proteins are required for the assembly or activity of both sensory and motile cilia [45,60–62]. Moreover, some ciliary proteins may also play a role in non-cilia-related processes [63]. In consequence, mutations in such genes cause complex body defects or even death. Single-celled models facilitate the analyses of the outcome of mutations in ciliary genes solely on the phenotype of the cell carrying the mutation. Changes in the phenotype of unicellular model organisms that manifest by altered swimming, cilia length, or motion (ciliary waveform, amplitude, and frequency) can be easily monitored using phase-contrast microscopy or dark-field microscopy combined with a high-speed camera as cilia are directly accessible. Furthermore, established microscopic techniques (transmission electron microscopy (TEM) and cryo-electron tomography (cryo-ET)) combined with methods of genome manipulation enable not only the analysis of cilia ultrastructural defects but also the precise localization of newly identified ciliary proteins. Finally, the maintenance of single-celled models is relatively easy and inexpensive, and a short generation time ensures the availability of a large volume of cultures and the purification of a sufficient amount of ciliary proteins for large-scale proteomic and biochemical analyses.

Equally important is the fact that the use of single-celled models is in agreement with the 3Rs principle—Replacement, Reduction, and Refinement—which was developed to minimize the number of consciously-living higher animals used in scientific experiments [64].

On the other hand, unicellular models and humans are evolutionarily distant species, and while some ciliary genes are highly conserved, other PCD-causative genes are less conserved or not present in the unicellular models' genomes. Moreover, many ciliary proteins are specific only to unicellular models, as was shown by the proteomic analyses of total ciliomes [65–67].

### 2.1. Green Alga, *Chlamydomonas reinhardtii*

*Chlamydomonas reinhardtii* is undoubtedly a splendid model organism for the study of many aspects of motile cilia/flagella assembly and functioning, and without a doubt, for a long time, *Chlamydomonas* was a leading model used by cell biologists to discover the identity, precise intraciliary localization, and the role of ciliary proteins. Subsequently, a lot of the genes encoding these proteins turned out to be the PCD-causative genes, and the knowledge gained during studies on green alga helped to understand the ultrastructural changes behind the cilia dysfunction in affected individuals, especially since the cryo-ET era began.

On the other hand, although the cilia ultrastructure, in general, is highly evolutionarily conserved, in *Chlamydomonas* flagella, in contrast to humans and other model organisms, only two radial spokes are full-length structures (RS1 and RS2), while RS3 is reduced to the short knob. Such truncation excludes direct interactions between RS3 and a central apparatus [68,69]. Thus, some differences in the regulation of *Chlamydomonas* flagella and human cilia beating cannot be excluded.

This small, oval-shaped green alga assembles two motile flagella that are longer (~10–14 µm) than the cell itself (Figure 2a) [70,71]. In the laboratory, *Chlamydomonas* can be grown in both liquid and solid media, and under optimal conditions and constant light it can multiply every 8–10 h [71,72]. Such a short generation time ensures that a large number of cells, and consequently a large amount of ciliary proteins, can be obtained in a relatively short time.

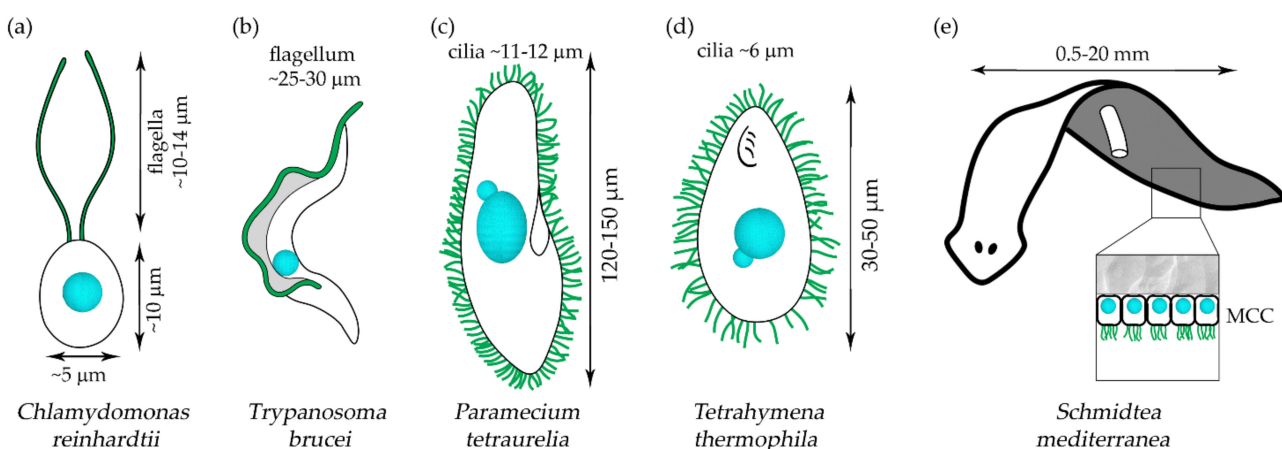


**Figure 2.** A schematic representation of the non-vertebrate PCD model organisms, the unicellular (a) Green alga *Chlamydomonas reinhardtii*; (b) Parasitic protist, *Trypanosoma brucei* (bloodstream-form) and two free-living ciliates, (c) *Paramecium tetraurelia* and (d) *Tetrahymena thermophila* as well as the multicellular (e) Freshwater planarian flatworm, *Schmidtea mediterranea*, with an enlarged fragment showing the multiciliated cells (MCCs) of the ventral epidermis. Nucleus (cyan), motile  $9 \times 2 + 2$  cilia/flagella (green).

*Chlamydomonas* cells are haploid; hence, mutations are immediately expressed, affecting cell phenotype and in the case of ciliary genes—flagella assembly and/or motion (worthy of note is the fact that old flagella are retracted before division, and new flagella are assembled based on the expression from a modified genome). *Chlamydomonas* mutants can be generated by exposure to UV radiation or chemical agents, or by insertional mutagenesis (random integration of DNA fragments containing a selectable marker (non-

homologous recombination), causing gene inactivation). Molecular mapping followed by rescue experiments or whole-genome sequencing enables the identification of mutated loci [73,74]. More importantly, mutations in different loci can be combined and expressed in a single cell by mating cells carrying particular mutations [75]. Conveniently, the libraries of *Chlamydomonas* insertional mutants are commercially available [76,77].

Not only forward genetics but also reverse genetic tools are well established for *Chlamydomonas*, and enable both the expression of recombinant proteins and gene silencing [73,74]. Genome editing, including knockout and knock-in, using the CRISPR/Cas9 approach (clustered regularly interspaced short palindromic repeats and CRISPR-associated protein 9) was also adopted [78–80], but as of yet, it is not broadly used. Recently, a modified, more efficient version known as TIM (targeted insertional mutagenesis) was proposed [81].

The DNA fragments can be delivered to the cell by several methods, including biolistic transformation, DNA-coated glass beads, and the most efficient and broadly used method—electroporation [75,82–87].

The well-established cell biology methods enable not only the analysis of ultrastructural changes in the cilia but also an investigation into how these structural changes translate into alterations in flagella movement and cell motility (from mild defects to cell paralysis) [88]. For example, *CCDC39/FAP59* and *CCDC40/FAP172*, whose mutations (next to mutations in genes that encode dynein arms) are frequent causes of PCD, were shown to form a filament that functions as a molecular ruler, marking not only the length of the 96 nm axonemal repeat but also a position of the main ciliary complexes such as IDAs, N-DRC, and RSs, but not ODAs [89]. The positioning/attachment of ODAs is affected by a product of *CCDC103*, another PCD-causative gene, as was also discovered in *Chlamydomonas* [90,91]. Studies conducted in green alga also revealed that PCD-related DRC1, 2, and 4 proteins form a core of the N-DRC, and that large parts of N-DRC are missing when genes encoding these proteins are mutated [92]. N-DRC is a main ciliary hub that coordinates and regulates other ciliary complexes of the 96-axonemal unit and connects adjacent outer doublets [92]. Using *Chlamydomonas* as a model, it was also shown for the first time that the *RSP3* gene encodes a component of the RS stem, and that the *RSP3* mutants lack the entire RS structure while the *RSP1*, 4, and 9 proteins build the RS head, and their lack affects only this part of the RS complex [68,69,93–95]. *FAP57/WDR65* is another PCD-causative gene [96], and the encoded protein forms a filament-like structure extending along the 96 nm axonemal unit, as was shown in *Chlamydomonas* [97]. Finally, *CPC1/SPEF2* [98], *FAP221/PCDP1* [99], *Hydin* [100], and *PF16/SPAG6* [101,102] (recently revealed to cause PCD [103]) were shown to encode components of the central apparatus structure, and mutations in these genes caused the lack of C1b-C1f, C1d, C2b-C2c, or C1a-c-e projections, respectively.

Besides early studies showing the significance of the structural components of dynein arms for flagella motility—such as dynein heavy chain, *oda2* [104], the two intermediate chains *IC78/IC1* and *IC69/IC2* [105,106] (orthologs of the human PCD-related genes *DNAH5*, *DNAI1*, and *DNAI2* [107–110])—*Chlamydomonas* was used as a model to verify the importance of genes that have recently been found to be mutated in patients having cilia without dynein arms. These genes encode cytoplasmic proteins required for dynein arm assembly: *CFAP298/FBB18* [111], *CFAP300/FBB5* [112], *DNAAF1/LRRC50/ODA7* [113–115], *DNAAF2/KTU/PF13* [114,116–118], *DNAAF3/PF22* [114,116,119], *DNAAF4/PF23/DYX1C1* [116,120], *HEATR2* [121], *MOT48/IDA10* [118,122]; or for transport—*LRRC56/ODA8* [123] (for review, see [124]).

Interestingly, in some patients with detected fertility and laterality defects, the respiratory problems were not reported or were mild and thus did not fulfill the PCD criteria (e.g., in individuals with mutations in the *CCDC19/CFAP45* and *WDR16/CFAP52* [22]). The basic studies conducted in *Chlamydomonas*, among others, revealed that proteins encoded by such genes are not components of the main ciliary complexes, and that their lack does not affect or mildly affects flagella motion (reduces beating frequency and/or amplitude and waveform). For example, the abovementioned *CFAP45* and *CFAP52* are microtubule-binding proteins attached to the inner (luminal) wall of the outer doublet

B-tubule and are likely stabilizing outer doublets [125]. Similarly, several genes recently shown to be MMAF-causative genes were identified as encoding proteins positioned near the radial spoke base or dynein arms. These are FAP61, FAP91, and FAP251 forming the CSC complex [34,35], the RS2-base protein, FAP206 [126], and FAP43 and FAP44, forming the tether/tetherhead complex positioned near the motor domains of the heterodimeric IDAf/I1 and regulating IDAf/I1 activity [127].

## 2.2. Parasitic Protists, *Trypanosoma* spp.

Trypanosomes are broadly studied, uniflagellated, parasitic protists that cause tropical diseases such as sleeping sickness (*T. brucei*) or Chagas disease (*T. cruzi*). Taking advantage of the collected general knowledge on the culture condition, genome modifications, and biology of Trypanosomes gained during the analyses of these parasites, researchers “converted” *Trypanosoma* spp. into a model to study PCD. *T. brucei* has a two-host multi-stage life cycle, and cells at different developmental stages vary in their size and flagellum length. In the so-called short epimastigote, which is the smallest of all *T. brucei* forms, the flagellum is only ~3 µm long. In metacyclic trypomastigotes and attached epimastigotes, the flagellum length ranges from 13 to 16 µm, while the procyclic form has ~20 µm flagella. The longest flagella (~25–30 µm) are assembled by the bloodstream slender form, long trypomastigotes, and long epimastigotes [128,129].

The flagellum (except for short epimastigote) is docked in the cell posterior end and extends parallel to the cell surface, in the direction of the cell anterior end and beyond it (Figure 2b). Most of the flagellum (more precisely, the flagellar membrane) is laterally connected to the cell by a membranous-cytoskeletal structure called a flagellar attachment zone (FAZ) formed by both flagellum and cell surface. The most distal, unattached part of the flagellum is short and comprises roughly one-tenth up to one-seventh of the entire flagellum length (at least in epimastigote-like cells) [130]. Besides the axoneme composed of typical for motile cilia components, Trypanosomes’ flagellum contains an additional, unique structure called the paraflagellar rod, extending along the axoneme length parallel to doublets 4–7 [131].

During cell division, old and newly assembled flagella co-exist until the daughter cells separate. Thus, in cells with knocked down ciliary genes, such a phenomenon provides an opportunity for comparing the ultrastructure and behavior of old unaffected flagellum and new flagellum formed after the elimination of the protein of interest. Hence, differences in the ultrastructure and motility between old and new flagella can be specifically attributed to the function of the targeted protein.

The procyclic stage (present in tsetse fly midgut) and bloodstream form of *Trypanosoma brucei* can be cultured in vitro, in both liquid and solid media. The average doubling time of the strain commonly used in the laboratory is approximately 6–8 h for the slender bloodstream form and 8–9 h for the procyclic form [132]. More importantly, both forms can be stored deep-frozen for a long time.

The available molecular tools enable the stable or transient expression of tagged proteins under the control of a native promoter or their overexpression, as well as gene silencing using a tetracycline-inducible RNAi system [132–134]. The DNA constructs can be introduced into the cell by the highly effective electroporation or by nucleofection [132,135–137] and efficiently incorporated into the genome via homologous recombination [132]. The recent adaptation of the CRISPR/Cas9 method expanded the repertoire of *Trypanosoma* genome manipulation [137–140]. The effect of the mutation or knockout of ciliary genes on cilia assembly or motion can be evaluated by the direct observation of the flagella movement and the analysis of the pattern of cell swimming using video microscopy, or less precisely, by the sedimentation assay [132,141–144]. At the ultrastructural level, not only classical SEM and TEM but also cryo-ET approaches were successfully applied [145–147].

Although to a lesser extent than *Chlamydomonas*, *Trypanosoma* was also used as a model in both basic studies aiming to discover the role of ciliary proteins (including those that were later shown to be implicated in PCD etiology) and in verifying that genes identified

as causative in PCD-affected individuals are indeed responsible for cilia/flagella motility alterations. For example, the knockdown of the component of motile flagella 70, CMF70, and *trypanin*, orthologs of DRC2 and DRC4, respectively, resulted in uncoordinated flagella beating that hardly translated into cell movement (similar as in patients with *DRC2* or *DRC4* mutations) [148,149]. The knockdown of *hydin* also significantly affected *Trypanosoma* cells' motility and caused ultrastructural changes such as the rotation of the central apparatus and the lack of one (7%) or both (19%) central microtubules [150]. Some flagella without one (5–12%) or both (3–5%) central microtubules were also observed in *Chlamydomonas hydin* mutants; however, the majority of *Chlamydomonas* flagella lacked C2b and a part of the C2c central apparatus projections [100]. It is likely that in *Trypanosoma* mutant flagella, the C2b projection was also missing, but structural defects were probably too subtle and thus not apparent in TEM images. In contrast, the knockdown of PF16/SPAG6 in *Trypanosoma*, another central apparatus protein, only led to the rotation of the central apparatus [142].

In *Trypanosoma*, as in other organisms, the knockdown of *RSP3* [142] affected radial spoke assembly and cell motility, while the formation of dynein arms was reduced in cells with knocked out genes encoding the dynein arm structural protein, *DNAI1* [143], dynein arm assembly factors (*DNAAF1/LRRC50/ODA7*) [113], or *LRRC56/ODA8*, a protein required for the transport of dynein arms to the distal part of the axoneme [151]. On the other hand, mutants with the knockdown of *TbLRTP* encoding a protein with some similarity to *LRRC6/DNAAF11* as suggested by [152] exhibited a different phenotype; while cilia in PCD-affected individuals carrying *LRRC6* mutation lack ODAs and IDAs [153], flagella of *Trypanosoma* cells with a reduced level of *TbLRTP* were described as having a normal ultrastructure (the presence or lack of dynein arms was not specifically addressed) [154]. Moreover, the cell proliferation rate was reduced in the *TbLRTP* mutant, thus casting doubt as to whether this is a true functional homolog of mammalian *LRRC6*.

*Trypanosoma* cells were also used as a model to elucidate the flagellar role of proteins encoded by the MMAF-causative genes. These were CFAP43 and CFAP44 [155], CFAP91 [156], CFAP251/WDR66 [157], and TTC29 [158]. Surprisingly, CFAP43 and CFAP44, which were shown to build small tether/tetherhead complex in *Chlamydomonas* and *Tetrahymena* [127], were found to be located between the paraflagellar rod and outer doublets 5 and 6 in *Trypanosoma* [155]. However, the localization of CFAP43 and CFAP44 in *Trypanosoma* was addressed using STED super-resolution microscopy, while the visualization of the tether/tetherhead complex in cilia and flagella of free-living model organisms was performed using cryo-ET. Thus, one cannot exclude that CFAP43 and CFAP44 have dual localization in *Trypanosoma*, near IDA f/I1 as in other ciliated organisms, and in *Trypanosoma*-specific organisms, between the paraflagellar rod and axonemal outer-doublets.

### 2.3. Ciliate: *Tetrahymena* and *Paramecium*

In contrast to *Trypanosoma* assembling a single flagellum or bi-flagellated *Chlamydomonas*, free-living, fresh-water organisms that belong to ciliates, *Tetrahymena* and *Paramecium* (Figure 2c,d), have several hundred cilia that enable cell locomotion (somatic cilia) or direct food particles into the oral cavity (oral cilia). *Tetrahymena thermophila* and two species of *Paramecium*, *P.tetraurelia*, and *P.caudatum*, are well-established laboratory models. In the natural environment, they feed on bacteria, but in the laboratory, these species can be maintained on axenic media. An interesting feature of ciliates is the presence of two types of nuclei, the generally transcriptionally silent diploid micronucleus and the transcriptionally active ampliploid macronucleus (not the entire genome is amplified) [159].

*Tetrahymena* is 30–50 µm long and forms ~600 cilia with the average length of ~6 µm. *Paramecium* is a larger ciliate (*P.tetraurelia* is 120–150 µm long, while *P.caudatum* is ~300 µm) and assembles ~4000–5000 cilia that are ~10–12 µm long [160–164]. When grown under optimal conditions, *Tetrahymena* divides every 2.5–3 h, while *Paramecium* requires twice as much time (*P.caudatum*, 7.6–8.4 h [165], *P.tetraurelia*, 5–14 h (depending upon culture conditions, including medium type) [166]). Short generation time and low-cost culture conditions, together with established methods of triggered cilia shedding followed by

their fast (~2 h) and synchronous regeneration, enable the large-scale biochemical studies of proteins in assembling and full-length cilia. Furthermore, the microscopic techniques enabling analyses at the cellular and ultrastructural levels are well-developed [167–172].

In the case of *Tetrahymena*, not only microscopic methods but also biochemical approaches and tools for reverse and forward genetics are well-developed. Appropriate constructs that enable gene deletion, mutagenesis, or protein tagging for localization studies (GFP, HA, V5) or biochemical experiments (BioID) can be introduced to the cell using biolistic transformation and be incorporated into the micro- or macronuclear genome via homologous recombination. The expression of fusion proteins can be controlled either by a native promoter or a cadmium-inducible metallothionein promoter, leading to protein overexpression [173–176].

While changes in the macronuclear genome affect cell phenotype, mutations in the micronucleus are “silent” and manifest after a sexual process (conjugation) when new macronuclei are formed based on the micronuclear genome of two conjugating cells. Such nuclear dualism is advantageous while investigating the role of essential genes as lethal mutations can be “stored” in micronuclei (and thus a mutated strain can be maintained) and expressed after conjugation [174,177].

Because ciliates use cilia for cellular motility and feeding, defects in cilia affect cells’ swimming phenotype (cell velocity, shape of swimming trajectories, ciliary beating pattern, amplitude, and/or frequency) and food particle uptake (phagocytosis). Both these processes can be monitored using light microscopy [167].

In comparison to *Tetrahymena*, there are fewer approaches enabling genome manipulation in *Paramecium*. For localization studies, constructs enabling the expression of GFP-tagged proteins are introduced to the macronucleus by microinjection. To silence gene expression (RNAi-based knockdown), *Paramecium* is usually fed with bacteria, but the microinjection of dsRNA is also possible [163,178,179]. Another challenge is *Paramecium* cells’ senescence and long-term storage.

Recently, it was demonstrated that the knockdown of ciliary genes in *Paramecium* causes defects similar to those observed in PCD-affected individuals. The deletion of the ortholog of human DNAH9, a dynein heavy chain that, together with DNAH5, are components of the ODAs in the distal part of the respiratory cilia [180,181], reduces the number of ODAs in *Paramecium* cilia [182]. Furthermore, cilia in *Paramecium* cells with the silenced expression of ZMYND10 (Zinc finger MYND-type containing 10) [183], TTC12 (Tetratricopeptide repeat protein 12) [184], or CFAP300/FBB5/C11orf70 [112] had a reduced number of outer and inner dynein arms. More importantly, individuals with PCD caused by mutations in ZMYND10 [185–187] or CFAP300 [112,188] showed similar ultrastructural defects in respiratory cilia, while mutations in TTC12 resulted only in the lack of IDAs [184]. Interestingly, in the same individuals carrying TTC12 mutations, sperm flagella lacked both IDAs and ODAs [184]. The localization studies of the GFP-tagged CFAP300, TTC12, and ZMYND10 proteins showed that they are generally cytoplasmic, and only limited amounts are present in cilia [182–184]. These observations are in agreement with data obtained in other models, showing that investigated proteins are involved in dynein arm assembly [189].

Although *Tetrahymena* has not yet been used as a model to investigate newly identified PCD-related genes, research conducted on *Tetrahymena* shed some light on the structure and protein composition of different ciliary complexes required for cilia assembly and cilia beating regulation. The knockout of SPEF2A, a PCD-related gene encoding a sub-unit of the central apparatus that is essential for the assembly/stability of the entire C1b projection, changes the pattern of cilia beating to one that is rotatory-like [172]. A similar effect was caused by the deletion of CFAP69 encoding another C1b protein [172]. Interestingly, in humans, mutations in genes orthologous to SPEF2A (SPEF2) and CFAP69 turned out to cause MMAF and very rarely PCD (until now, only mutations in SPEF2 were connected to PCD) [190–195]. Among other MMAF-causative genes [196,197] studied in *Tetrahymena* are, as mentioned before, CFAP43 and CFAP44 [127,198–202], the CSC subunits

*CFAP61* [203,204] and *CFAP251* [204,205], and *CFAP206*, which forms a part of the RS2 base [126,196].

The presented examples clearly show how the detailed analyses at the molecular, ultrastructural, and proteomic levels conducted in single-celled models help to understand the cilia-related changes observed in PCD patients.

### 3. Freshwater Planarian *Schmidtea mediterranea*—Matters Becoming a Little More Complicated

Although single-celled organisms are convenient models for the exploration of various aspects of cilia biology, certain questions regarding cilia assembly, beating regulation, and coordination cannot be addressed. A free-living planarian, *Schmidtea mediterranea*, used for over 100 years to investigate the regeneration process [206], has recently emerged as a model for the study of de novo centriole formation, planar cell polarity as well as motile cilia assembly and functioning [188,207–210]. As the name of the phylum suggests (flatworms, Platyhelminthes), the body of *Schmidtea* is flat and thin (Figure 2e). The adult form is ~20 mm long (the asexual strain is slightly smaller); however, under starvation conditions, the body size can be reduced to ~0.5 mm. The epithelial multiciliated cells (MCCs) of the ventral epidermis assemble classical motile cilia (~80 per cell) that mediate animal locomotion [207,211]. MCCs are also present in the epithelium lining a pharynx, the planarian feeding organ [208], and in protonephridia, the planarian excretory system where they are called “flame cells” [212,213]. Additionally, in auricles, structures participating in both chemo- and mechano-reception among ciliated epithelial cells are sensory neurons, assembling cilia with classical 9 × 2 + 2 microtubule organization, (however, it is unknown if those cilia are motile [214]). Because planarian MCCs share many features with vertebrate MCCs, data regarding basal body biogenesis and ciliogenesis obtained using *Schmidtea* as a model can shed a light on these processes in MCCs present in epithelia lining airways, brain ventricles, or oviduct in humans [215].

Although the repertoire of methods, especially those enabling genome manipulations in *Schmidtea*, is limited in comparison to those available for single-celled models, the planarian offers several advantages. Compared to vertebrate models, *Schmidtea* culture is simple and inexpensive as planarians can be maintained at 18–20 °C in the dark, in plastic, food-grade containers with an inorganic medium composed of common salts, and then fed once a week with calf liver homogenate. Before the experiment, a larger number of planarians can be obtained either by animal fission or by manual amputations, followed by the regeneration of obtained body fragments. Importantly, progenies obtained from a single animal, either by subsequent fissions or amputations, have the same genetic background, which is crucial while comparing control and experimental animals [216,217].

Methods enabling the expression of mutated or tagged proteins in *Schmidtea* are not yet available, but RNA interference (RNAi)-based gene knockdown is straightforward and efficient. RNAi can be introduced into planarian cells either by the microinjection of long double-stranded RNAs (dsRNA) or by feeding with an *E. coli* strain carrying a plasmid for dsRNA expression [211,218]. The amputation of the part of the planarian body ensures that MCCs in the regenerating fragment will lack or have a low level of expression of the targeted gene. The effect of the gene depletion can usually be observed in less than a week [211,218,219].

Similar to unicellular models, cilia assembled by planarian ventral epidermis and pharynx are easily accessible, and thus the effect of gene silencing on cilia assembly/functioning and subsequently planarian locomotion can be observed without difficulty. The ciliary waveform, beating frequency, and synchrony of cilia beating can be analyzed after recording the movement of cilia in the lateral part of the animal using a high-speed video camera and differential interference contrast (DIC) microscopy [219]. Changes in planarian locomotion can be described by measuring the speed of animal movement. The effect of gene silencing on cilia protein composition and ultrastructure can be revealed using the methods of immunofluorescence and electron microscopy, respectively [211,218,219].

Until now, only a limited number of proteins encoded by cilia-related genes has been studied using *Schmidtea* as a model. These are (i) FoxJ1-4, one of the key transcription factors controlling ciliogenesis in MCC cells [220], (ii) CFAP298/FBB18 [11] and CFAP300/FBB5/C11orf70 [188], the PCD-causative genes encoding cytoplasmic proteins that participate in dynein arm assembly/transport [112,188,221], (iii) DAW1/WDR69/ODA16 [209], an adaptor protein involved in outer dynein arm transport [222–224], not yet linked to PCD but likely a causative gene based on ultrastructural defects (reduced number of ODAs) in *Chlamydomonas* [225], zebrafish [226], and mouse [227] mutants, and (iv) CFAP45/CCDC19/NESG1 and CFAP52/WDR16 [22], two proteins that were shown to localize in the lumen of the outer doublet B-tubule in *Chlamydomonas* [125]. In humans, as mentioned above, mutations in either *CFAP45* or *CFAP52* cause mild respiratory distress, although without fulfilling the PCD diagnosis criteria. The affected individuals develop situs inversus and asthenospermia [22]. Importantly, in the case of all these proteins, their knockdown in *Schmidtea* affected cilia motility as in other model organisms. Thus, with the further development of tools for reverse genetics, it is likely that the planarian will become a valuable and popular PCD model.

#### 4. Aquatic Vertebrates—When a Plethora of Siblings and Fast Development Matter

As stated above, single-celled organisms and to less extent, a free-living flatworm, are convenient models to investigate the role of ciliary genes, including those related to PCD. However, certain motile cilia-related genes and processes (especially genes controlling embryo's laterality or development and functioning of cilia-bearing organs) obviously cannot be studied in unicellular organisms or in planarian but require the employment of vertebrate models.

Embryos of zebrafish (*Danio rerio*) and two species of *Xenopus*, the South African clawed frog, *X. laevis* and smaller Western clawed frog, *X. tropicalis*, are well-established models to study diverse biological processes, including those involving motile cilia (Figure 3). Both these aquatic vertebrates produce a huge number of oocytes that after external fertilization develop outside of the mother's body, enabling direct observations of the outcome of cilia activity and defects caused by cilia dysfunction in a reliable number of animals.

Zebrafish females reach sexual maturity after about three months and weekly can lay even 100–300 eggs (with a diameter ~0.7 mm) [228,229]. *Xenopus* species require at least twice that time to reach the sexual maturity—5.5–7.5 months post-metamorphosis (PM, a transition from a tadpole to adult form that usually takes place within 2–3 months after fertilization) in the case of *X. tropicalis* and 10–24 months PM in the case of *X. laevis* [230]. *Xenopus* females lay more than 1000 eggs per mating [231], and similar to zebrafish, oocytes are large (~1.3 mm in *X. laevis* and 0.8 mm in *X. tropicalis*) [232]. In contrast to diploid *X. tropicalis*, the genome of the *X. laevis* has undergone duplication and is hence tetraploid, making genetic manipulations difficult. Thus, larger embryos of the *X. laevis* are preferentially used in microscopic or transplantation studies, while genome modifications are performed in *X. tropicalis* embryos [233–235].

In both zebrafish and *Xenopus*, motile cilia appear early in the embryonic development. In zebrafish embryos, motile cilia are first formed in the lumen of a transient, fluid-filled structure homologous to mammalian node, the left-right organizer, LRO, called a Kupffer's vesicle (KV). KV is present in embryos at 4–14 somite stages (~11–18 hpf, hours postfertilization) and is involved in establishing the left-right body organs' asymmetry. Interestingly, not all KV's cilia are motile. The number of motile cilia increases, and the pattern of fluid flow changes as KV's development advances. Thus, cilia motion in the KV is usually studied in embryos at 6–10 somite stages [228,236–238]. Both motile and immotile cilia are assembled as a single structure per cell, and at 8-somite stage, their length has been estimated to be ~3.3 µm in fixed embryos [236] and from 4 to 12 µm (on average, 6–8 µm) when cilia were imaged in live or fixed embryos [237].

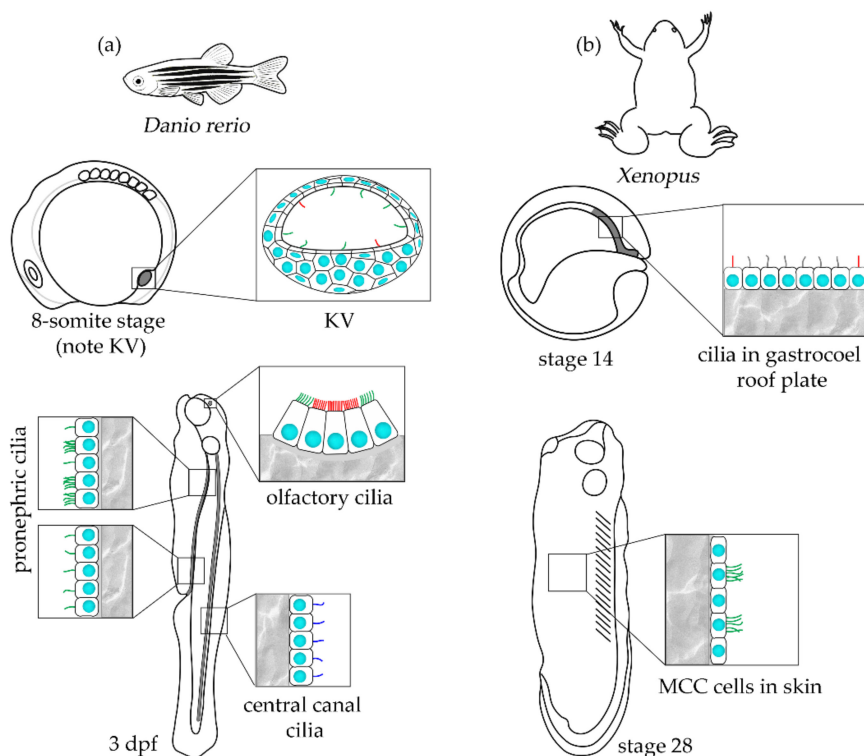


**Figure 3.** A schematic representation of the larval and adult forms of vertebrate PCD models, (a) zebrafish and (b) *Xenopus*. The adult animals reach the following sizes: zebrafish ~3.5 cm; *X. laevis*, males between 4.5 and 9.8 cm, females from 5.7 to 14.7 cm; *X. tropicalis*, males between 3.2 and 3.9 cm, females between 4.8 and 5.5 cm ([https://zfin.org/zf\\_info/zfbook/stages/](https://zfin.org/zf_info/zfbook/stages/) accessed on 30 December 2021 [239], <http://www.xenbase.org> accessed on 30 December 2021 [240]). Nuclei (cyan), motile  $9 \times 2 + 2$  cilia (green), motile  $9 \times 2 + 0$  central canal cilia (navy blue), immotile cilia (red), motile cilia in gastrocoel roof plate of unknown microtubule configuration (grey).

As zebrafish larvae further grow (approximately 24–72 hpf larvae are ~1.2–1.7 mm long), motile cilia are formed in the olfactory placode, pronephros, brain ventricles, and spinal central canal [236,241]. Cilia in the spinal canal lumen, similar to cilia in the KV, are assembled as a single structure per cell and exhibit rotational movement, but in contrast to the KV where the vast majority of cilia have  $9 \times 2 + 2$  microtubule organization [237,242], cilia in the spinal canal show a  $9 \times 2 + 0$  microtubule pattern [236]. Their rotational motion contributes to the cerebrospinal fluid flow [236]. Cilia in spinal central canal are ~2.1  $\mu\text{m}$  [236].

Epithelial cells lining pronephric ducts can be both mono- and multiciliated, and cilia reach ~8.8  $\mu\text{m}$  [236]. Mono- and multiciliated cells are present in the anterior and middle part of the pronephric ducts, while in the posterior part, cells are mostly monociliated [236,243,244]. It is worth pointing out that monocilia are formed earlier (~24 hpf) than cilia in multiciliated cells (~2 days) [244].

Cells of the olfactory placode assemble both, sensory and motile cilia. The latter ones are assembled as multicia, mainly by cells at the olfactory placode periphery [242].

Zebrafish embryos with mutations in ciliary genes develop apparent phenotypic changes such as ventral body curvature, hydrocephalus, and pronephric swellings or formation of kidney cysts. A more detailed examination can also reveal abnormal otolith deposition and altered left-right body asymmetry, including random heart jogging and looping [245,246].

Similar as in zebrafish embryos, motile cilia in *Xenopus* embryos, are first formed as monocilia in the transient structure called the gastrocoel roof plate, playing the role of the left-right organizer [247,248]. LRO cilia start to assemble at stage 14 (~16 hpf) and at

stage 16–18 (~18–20 hpf), approximately 250–270 cilia of ~5–6  $\mu\text{m}$  beat rotationally, causing leftward fluid flow ([249,250], <https://www.xenbase.org/anatomy/alldev.do> accessed on 30 December 2021). Cells assembling motile cilia are bordered by cells forming non-motile cilia [247]. The effect of LRO cilia activity (position of developing heart and other organs) can be analyzed in 3–4 days old larvae [248,251].

In *Xenopus*, motile cilia formed by the larva and tadpole skin (stages 20–50, larvae hatch at the stages 35–36) are the most often studied cilia [252]. They are assembled as multiple, polarized structures (~150 per cell [253]) with the length of ~18–20  $\mu\text{m}$  [254] and support the flow of egg liquid, or, after hatching, of water along the skin surface. Besides multiciliated cells, epithelium of larvae skin contains several other non-ciliated cell types: mucus-secreting cells, ionocytes, proton secreting cells, and small secretory cells [255], and thus has a composition which is highly similar to the mammalian airways epithelium (although these epithelia are derived from different germ layers). Cells destined to become multiciliated start to express cilia-specific genes ~12 hpf (stage 11.5), and ciliogenesis starts around stage 20 (~21 hpf). By stage 28 (~32 hpf), assembled cilia are properly oriented [251,256,257].

Motile cilia are also formed in the otic vesicle and by the tadpole floor plate of the spinal cord (monocilia) as well as in brain ventricles (ependymal, mono- and multiciliated cells, forming ~4–9  $\mu\text{m}$  long cilia) 3–4 days after fertilization. They support the circulation of the cerebrospinal fluid [255,258]. Similar to zebrafish, ciliary defects in *Xenopus* embryos can cause laterality defects and hydrocephalus.

In contrast to mice embryos, in zebrafish or *Xenopus* embryos, cilia are either directly accessible (epidermis, olfactory cilia) or visible because of the embryo's body transparency (e.g., cilia in KV or pronephros). Thus, the cilia motion can be observed in living embryos. The efficiency of cilia beating can be monitored by tracing the movement of fluorescent beads injected into zebrafish embryo's KV at 6–10 somite stages or *Xenopus* embryo's gastrocoel roof plate at stage 17 or into brain ventricles at stage 46 [238,248,258]. Cilia motility in pronephros, spinal canal, olfactory placode (zebrafish) or skin (*Xenopus*), and the estimation of cilia length can also be conducted in living transgenic embryos expressing GFP-tagged ciliary proteins such as Arl13b, or by injection of mRNA encoding GFP-tagged ciliary protein [245,259,260].

As mentioned above, the large size of the zygotes and blastomeres of early embryos facilitates the relatively easy introduction of the DNA, mRNA, morpholino, proteins, or drugs into developing embryo, providing convenient tools for the study of cilia assembly and function [233,235,245,260]. Injection of morpholino (MO), a very stable artificial oligonucleotide complementary to mRNA translation start or splice junction, enables efficient gene knockdown. However, the morpholino has to be carefully validated as it may cause toxicity and off-target effects, the issues that can be resolved by the co-injection of mRNA encoded by the targeted gene (rescue experiment) [261]. More recently developed methods involving the transcription activator-like effector nuclease (TALEN) and CRISPR/Cas9 approaches enable gene knockout [262,263]. Particularly noteworthy is the fact that an increasing number of studies has reported the differences in the phenotype of gene morphant and mutant. Bases for such a phenomenon were broadly discussed in a recently published review [264].

Owing to the fact that zebrafish embryos with silenced expression or a mutation of the ciliary genes exhibit characteristic developmental abnormalities, this model organism has been frequently used to investigate the significance of PCD-causative genes. The zebrafish homologs of human PCD-causative genes were listed in a very recent publication [242]. Studies using zebrafish as a model not only reproduced ciliary defects observed in PCD-affected individuals but also helped to understand the molecular basis of such defects. Among PCD-related genes functionally studied in zebrafish embryos are genes encoding (i) factors required for cilia assembly and cell polarity: Foxj1 homologs [265,266], and MCIDAS/multicilin [267], (ii) cytoplasmic proteins required for dynein arm assembly (see Table 1 in [152] for a full list and references), (iii) proteins required for ODA docking:

CCDC151 [268], ARMC4 [269], TTC25 [270], CCDC103 [91], (iv) a molecular ruler protein CCDC40 [271], N-DRC subunits CCDC65/DRC2 [111] and GAS8/DRC4 [272,273], radial spoke components RSPH9 [94,274] and NME5 (Nucleoside diphosphate kinase 5) [275], and central pair-associated protein STK36/Fu [276].

Interestingly, with the recent use of zebrafish as a model, it was shown that CCDC103, the protein associated with axonemal outer doublets, is also present in myeloid cells where it co-localizes with microtubules. Mutations in *CCDC103* or *SPAG6* reduce microtubule stability and myeloid cell proliferation and migration [277]. Myeloid cells do not assemble cilia [278], but surprisingly, some researchers reported that myeloid cells obtained from PCD-affected individuals have some functional alterations [279–281].

In comparison to zebrafish, *Xenopus* embryo is a less frequently used model. A vast majority of PCD-causative genes studied in *Xenopus* encoded proteins involved in cilogenesis and cell polarity control. Those were *FOXJ1* [258,266], *MCIDAS/Multicilin* [282], *CCNO* [283,284], and *GAS2L2* [48]. Out of the two studied dynein arms-assembly proteins, *ZMYND10* and *CFAP298/FBB18/kurly*, only *kurly* morphants assembled multiple cilia with motility defects (additionally, also cell polarity was affected) [285], while *ZMYND10* morphants failed to form cilia despite the presence of numerous centrioles [185]. However, the rescue experiment was not included in this study; thus, it is not clear if the observed phenotype was specific. Moreover, the knockdown of *TTC25* in *Xenopus*, similar to zebrafish, mice, and humans, caused the lack of the outer dynein arms and laterality defects [250,254,270]. Finally, the significance of *CFAP43*, an MMAF-related gene, was also studied in *Xenopus* [286].

Ideally, animal models used to study human diseases should imitate or resemble humans in their genetic and physiologic characteristics. Thus, some types of experiments have to be conducted using mammalian models or in vitro cultured cells or tissues (either ones that are commercially available or derived from cells obtained from PCD-affected individuals). However, even these models have their pros and cons.

## 5. Mice—Blood Is Thicker Than Water—When Being a Mammal Matters

For more than 100 years, the mouse *Mus musculus* has been the most frequently used model organism. It is a truism that among all model organisms used to study PCD-related genes and the impact of their mutations on cilia assembly, structure, and motility, the mouse genome, development, and body organization are the most similar to those of humans [55,287–290]. Compared to other mammals, the maintenance of this small rodent is comparatively inexpensive, pregnancies are frequent (5–10 times per year), the gestation period is short (~19–20 days), and offspring are relatively numerous (on average 6–8 pups) [287,290,291]. It is also worth adding that mouse multiciliated cells such as mouse tracheal epithelial cells (mTEC) [292,293] or ependymal cells [294–296] can be cultured in vitro.

More importantly, cell biology, biochemistry, and molecular biology methods (both forward and reverse genetic approaches) are remarkably well-developed. The outcome of mutations in PCD-causative genes were studied in mutant mice obtained by (i) N-ethyl-N-nitrosourea mutagenesis (ENU) followed by a forward genetic screen (e.g., *Dnah5* [227,297] *Dnah11* [298,299], *Armc4* [269], *Ccdc39* [227,300], *Ccdc40* [271], *Ccdc151* [268], *Dnaaf1/Lrrc50* [301], and *Spef2* [302]), or reverse genetic approaches, including (ii) knockout mouse generated by traditional gene targeting (gene eliminated in all body cells), e.g., *Dnaaf2/Ktu* [303,304], *Rspf1* [305], and *Dnaaf4/Dyx1c1* [306], or more advanced (iii) conditional knockouts (inactivation of the gene in specific cell types in a certain tissue), e.g., *Spef2* [307,308], or (iv) CRISPR/Cas9 gene editing, e.g.: *Ttc25* [254], *Zmynd10/Dnaaf7* [189], *Dnajb13* [309], and *Mcidas* [310]. It should also be noted that mouse lines facilitating further genetic manipulations and the analysis of ciliated cells have recently been generated [311,312]. Finally, genetic manipulations of PCD-causative genes and their outcome can be analyzed in vitro using mouse tracheal epithelial cells (mTECs) [282].

The activity and/or structure of cilia in MCCs can be evaluated in vivo, ex vivo, or in vitro using radioactive particles, fluorescent beads, or lead dust and different, sophisticated microscopic systems [17,227,313–318].

Although motile cilia are present in mice and humans in the same organs, the phenotypic outcome of the mutation of PCD-causative genes is not identical. Mice carrying a mutation in ciliary genes frequently develop hydrocephalus, while in PCD-affected patients, such a condition is very rare. This striking discrepancy is likely due to anatomical differences between murine and human brain ventricles and additional specific genetic modifiers that segregate in inbred mouse strains, as was earlier suggested [287,319–321].

Without a doubt, over the years, research conducted using the mouse model has brought significant progress regarding genes and molecular mechanisms underlying PCD and motile ciliary function. These data were brought together recently in a splendid review article [287]. Therefore, we omit discussing this aspect here.

## 6. In Vitro Cell Culture

Assessment of cilia motion and ultrastructure are important tools in PCD diagnosis. However, the quality of samples obtained during biopsies is often poor due to secondary changes caused by infections or sampling itself. In consequence, the diagnosis can be challenging [322]. Moreover, the amount of the biological material obtained from the patient may not be sufficient to conduct all currently available tests. The culturing of cells collected during the nasal brushing or biopsy can overcome these problems and improve the diagnosis. More importantly, such cell culture “models” are patient-specific [323–325].

The airway epithelium is composed of several cell types, including progenitor basal cells, club cells, goblet cells, and multiciliated cells (for details, see [47]). Ciliated cells account for 50–70% of the epithelial cell population [326]. Basal cells bear an important feature - during asymmetric division, one of daughter cells maintains stem cell’s properties while the other one differentiates. Basal cells bear an important feature—during asymmetric division, one of the daughter cells maintains stem cell properties while the other one differentiates.

In vitro, cell differentiation and ciliation take place when cultured cells are attached to the floating collagen, form floating spheroids, or are grown under conditions that expose the apical part of the cell culture to air (air-liquid interface, ALI) [323,325,327–330]. A full differentiation of such cultured airway epithelium takes approximately 3–4 weeks [331]. Differentiated cultures can be maintained for more than several weeks or even months.

Obviously, cultures of cells derived from affected individuals and differentiating into airway-like epithelium are the most adequate tool for accurate understanding ciliary defects in PCD patients. However, in comparison with other PCD models, airway epithelial cell cultures are significantly more expensive and, because of limited availability of material, can be used only in several test types (e.g., light and electron microscopy, low-cell-number or single-cell analyses).

Up to now, ALI cultures have been used to support the analysis of PCD-causing mutations, including the mutation in *CFAP300/C11orf70* [221], *CCDC65* [332], *DNAH9* [333], *DNAH5* [334], *HYDIN*, [335], and *FOXJ1* [336].

The determination of conditions that enable the reprogramming of somatic cells into induced pluripotent stem cells (iPSC) (for review, see [337]) and the induction of the iPSC differentiation into mature multiciliated cells [338] are the next significant step forward in PCD-related research. In fact, several research groups have reported the establishment of human iPSCs (hiPSCs) from somatic cells of patients with primary ciliary dyskinesia carrying mutations in *CCDC40* [339], *DNAH5* [340], *NME5* [341], *CCNO* [342,343]. Another research group moved a step further and showed that iPSCs can be differentiated into airway basal cells, resembling those in the airway epithelium [344,345].

More importantly, the generation of patient-derived iPSCs and their differentiation into airways epithelium, together with genome editing technologies, represent a major tool for developing personalized PCD therapies in future.

## 7. Conclusions

Without a doubt, the research conducted using unicellular and multicellular model organisms has brought about enormous progress in our understanding of molecular, proteomic, and ultrastructural bases of cilia assembly and functioning, and has thus helped to elucidate ciliary abnormalities in PCD-affected individuals, and to consider novel genes as putative PCD-causative. Moreover, studies in the vertebrate models have shed light on some aspects of tissue and organ development. However, even such a closely related model as that of the mouse is not ideal for studying all aspects of PCD and successfully developing appropriate therapies. The situation is even more complicated as PCD is a heterogeneous disorder, and some PCD patients have more acute symptoms, while others have milder ones, depending on the mutated gene or even the type and position of the mutation in the same gene. On the other hand, the entire genetic background of the affected individual may also matter. The recent progress in the methods of hiPSC culture and their reprogramming give hope for the development of personalized therapies and drug testing.

**Author Contributions:** The authors (M.N., M.B., A.O., Z.S., J.S., M.P., R.B., H.F., E.J., D.W.) wrote particular sections of the original draft; reviewing and editing, E.J. and D.W.; drawings, E.J. All authors have read and agreed to the published version of the manuscript.

**Funding:** This research was funded by (i) the National Science Centre, Poland Grants: OPUS13 2017/25/B/NZ3/01609 to D.W. and OPUS15 2018/29/B/NZ3/02443 to E.J. and (ii) Project No. POWR.03.02.00-00-I007/16-00 implemented under the Operational Program Knowledge Education Development 2014–2020 co-financed from the European Social Fund Project NCBiR No. PBS3/A8/36/2015.

**Institutional Review Board Statement:** Not applicable.

**Informed Consent Statement:** Not applicable.

**Data Availability Statement:** Not applicable.

**Conflicts of Interest:** The authors declare no conflict of interest.

## References

1. Anvarian, Z.; Mykytyn, K.; Mukhopadhyay, S.; Pedersen, L.B.; Christensen, S.T. Cellular signalling by primary cilia in development, organ function and disease. *Nat. Rev. Nephrol.* **2019**, *15*, 199–219. [[CrossRef](#)] [[PubMed](#)]
2. Ford, M.J.; Yeyati, P.L.; Mali, G.R.; Keighren, M.A.; Waddell, S.H.; Mjoseng, H.K.; Douglas, A.T.; Hall, E.A.; Sakae-Sawano, A.; Miyawaki, A.; et al. A Cell/Cilia Cycle Biosensor for Single-Cell Kinetics Reveals Persistence of Cilia after G1/S Transition Is a General Property in Cells and Mice. *Dev. Cell* **2018**, *47*, 509–523.e5. [[CrossRef](#)] [[PubMed](#)]
3. Wensel, T.G.; Zhang, Z.; Anastassov, I.A.; Gilliam, J.C.; He, F.; Schmid, M.F.; Robichaux, M.A. Structural and molecular bases of rod photoreceptor morphogenesis and disease. *Prog. Retin. Eye Res.* **2016**, *55*, 32–51. [[CrossRef](#)] [[PubMed](#)]
4. Wensel, T.G.; Potter, V.L.; Moye, A.; Zhang, Z.; Robichaux, M.A. Structure and dynamics of photoreceptor sensory cilia. *Pflugers Arch. Eur. J. Physiol.* **2021**, *473*, 1517–1537. [[CrossRef](#)] [[PubMed](#)]
5. Falk, N.; Lösl, M.; Schröder, N.; Gießl, A. Specialized cilia in mammalian sensory systems. *Cells* **2015**, *4*, 500–519. [[CrossRef](#)]
6. Wang, D.; Zhou, J. The Kinocilia of Cochlear Hair Cells: Structures, Functions, and Diseases. *Front. Cell Dev. Biol.* **2021**, *9*, 2134. [[CrossRef](#)] [[PubMed](#)]
7. Jenkins, P.M.; McEwen, D.P.; Martens, J.R. Olfactory cilia: Linking sensory cilia function and human disease. *Chem. Senses* **2009**, *34*, 451–464. [[CrossRef](#)]
8. Breeze, R.G.; Wheeldon, E.B. The cells of the pulmonary airways. *Am. Rev. Respir. Dis.* **1977**, *116*, 705–777. [[CrossRef](#)]
9. Jafek, B.W. Ultrastructure of human nasal mucosa. *Laryngoscope* **1983**, *93*, 1576–1599. [[CrossRef](#)]
10. Bustamante-Marin, X.M.; Ostrowski, L.E. Cilia and mucociliary clearance. *Cold Spring Harb. Perspect. Biol.* **2017**, *9*, 1–17. [[CrossRef](#)]
11. Rodriguez, K.; Gaston, B.; Wasman, J.; Marozkina, N. Lessons From Unilateral Loss of Cilia: Early Nasal Nitric Oxide Gas Mixing and the Role of Sinus Patency in Determining Nasal Nitric Oxide. *Clin. Med. Insights Ear Nose Throat* **2017**, *10*, 117955061774636. [[CrossRef](#)] [[PubMed](#)]
12. Mirzadeh, Z.; Kusne, Y.; Duran-Moreno, M.; Cabrales, E.; Gil-Perotin, S.; Ortiz, C.; Chen, B.; Garcia-Verdugo, J.M.; Sanai, N.; Alvarez-Buylla, A. Bi- and uniciliated ependymal cells define continuous floor-plate-derived tanyctytic territories. *Nat. Commun.* **2017**, *8*, 13759. [[CrossRef](#)]
13. Lorencova, M.; Mitro, A.; Jurikova, M.; Galfiova, P.; Mikusova, R.; Krivosikova, L.; Janegova, A.; Palkovic, M.; Polak, S. Ependymal cells surface of human third brain ventricle by scanning electron microscopy. *Bratislava Med. J.* **2020**, *121*, 437–443. [[CrossRef](#)] [[PubMed](#)]

14. Bruni, J.E.; Montemurro, D.G.; Clattenburg, R.E.; Singh, R.P. A scanning electron microscopic study of the ependymal surface of the third ventricle of the rabbit, rat, mouse and human brain. *Anat. Rec.* **1972**, *174*, 407–419. [[CrossRef](#)] [[PubMed](#)]
15. Worthington, W.C.; Cathcart, R.S. Ependymal cilia: Distribution and activity in the adult human brain. *Science* **1963**, *139*, 221–222. [[CrossRef](#)]
16. Lyons, R.A.; Saridogan, E.; Djahanbakhch, O. The reproductive significance of human Fallopian tube cilia. *Hum. Reprod. Update* **2006**, *12*, 363–372. [[CrossRef](#)]
17. Wang, S.; Burton, J.C.; Behringer, R.R.; Larina, I. V In vivo micro-scale tomography of ciliary behavior in the mammalian oviduct. *Sci. Rep.* **2015**, *5*, 13216. [[CrossRef](#)]
18. Hoque, M.; Chen, D.; Hess, R.A.; Li, F.Q.; Takemaru, K.I. CEP164 is essential for efferent duct multiciliogenesis and male fertility. *Reproduction* **2021**, *162*, 129–139. [[CrossRef](#)]
19. Yuan, S.; Liu, Y.; Peng, H.; Tang, C.; Hennig, G.W.; Wang, Z.; Wang, L.; Yu, T.; Klukovich, R.; Zhang, Y.; et al. Motile cilia of the male reproductive system require miR-34/miR-449 for development and function to generate luminal turbulence. *Proc. Natl. Acad. Sci. USA* **2019**, *116*, 3584–3593. [[CrossRef](#)]
20. Ma, C.; Wu, H.; Zhu, D.; Wang, Y.; Shen, Q.; Cheng, H.; Zhang, J.; Geng, H.; Liu, Y.; He, X.; et al. Bi-allelic mutations in MCIDAS and CCNO cause human infertility associated with abnormal gamete transport. *Clin. Genet.* **2021**, *100*, 731–742. [[CrossRef](#)]
21. Terré, B.; Lewis, M.; Gil-Gómez, G.; Han, Z.; Lu, H.; Aguilera, M.; Prats, N.; Roy, S.; Zhao, H.; Stracker, T.H. Defects in efferent duct multiciliogenesis underlie male infertility in GEMC1-, MCIDAS- or CCNO-deficient mice. *Development* **2019**, *146*, dev162628. [[CrossRef](#)] [[PubMed](#)]
22. Dougherty, G.W.; Mizuno, K.; Nöthe-Menchén, T.; Ikawa, Y.; Boldt, K.; Ta-Shma, A.; Aprea, I.; Minegishi, K.; Pang, Y.P.; Pennekamp, P.; et al. CFAP45 deficiency causes situs abnormalities and asthenospermia by disrupting an axonemal adenine nucleotide homeostasis module. *Nat. Commun.* **2020**, *11*, 5520. [[CrossRef](#)] [[PubMed](#)]
23. Aprea, I.; Nöthe-Menchén, T.; Dougherty, G.W.; Raidt, J.; Loges, N.T.; Kaiser, T.; Wallmeier, J.; Olbrich, H.; Strünker, T.; Kliesch, S.; et al. Motility of efferent duct cilia aids passage of sperm cells through the male reproductive system. *Mol. Hum. Reprod.* **2021**, *27*, 1–15. [[CrossRef](#)]
24. Nonaka, S.; Tanaka, Y.; Okada, Y.; Takeda, S.; Harada, A.; Kanai, Y.; Kido, M.; Hirokawa, N. Randomization of left-right asymmetry due to loss of nodal cilia generating leftward flow of extraembryonic fluid in mice lacking KIF3B motor protein. *Cell* **1998**, *95*, 829–837. [[CrossRef](#)]
25. Wallmeier, J.; Nielsen, K.G.; Kuehni, C.E.; Lucas, J.S.; Leigh, M.W.; Zariwala, M.A.; Omran, H. Motile ciliopathies. *Nat. Rev. Dis. Prim.* **2020**, *6*, 77. [[CrossRef](#)]
26. Serres, C.; Escalier, D.; David, G. Ultrastructural morphometry of the human sperm flagellum with a stereological analysis of the lengths of the dense fibres. *Biol. Cell* **1983**, *49*, 153–161. [[CrossRef](#)]
27. Touré, A.; Martinez, G.; Kherraf, Z.E.; Cazin, C.; Beurois, J.; Arnoult, C.; Ray, P.F.; Coutton, C. The genetic architecture of morphological abnormalities of the sperm tail. *Hum. Genet.* **2021**, *140*, 21–42. [[CrossRef](#)]
28. Shinohara, K.; Hamada, H. Cilia in left-right symmetry breaking. *Cold Spring Harb. Perspect. Biol.* **2017**, *9*, 1–9. [[CrossRef](#)]
29. Gonçalves, J.; Pelletier, L. The ciliary transition zone: Finding the pieces and assembling the gate. *Mol. Cells* **2017**, *40*, 243–253. [[CrossRef](#)]
30. Reiter, J.F.; Leroux, M.R. Genes and molecular pathways underpinning ciliopathies. *Nat. Rev. Mol. Cell Biol.* **2017**, *18*, 533–547. [[CrossRef](#)]
31. Kiesel, P.; Alvarez Viar, G.; Tsoty, N.; Maraspin, R.; Gorilak, P.; Varga, V.; Honigmann, A.; Pigino, G. The molecular structure of mammalian primary cilia revealed by cryo-electron tomography. *Nat. Struct. Mol. Biol.* **2020**, *27*, 1115–1124. [[CrossRef](#)]
32. Osinka, A.; Poprzeczko, M.; Zielinska, M.M.; Fabczak, H.; Joachimiak, E.; Włoga, D. Ciliary Proteins: Filling the Gaps. Recent Advances in Deciphering the Protein Composition of Motile Ciliary Complexes. *Cells* **2019**, *8*, 730. [[CrossRef](#)] [[PubMed](#)]
33. Heuser, T.; Barber, C.F.; Lin, J.; Krell, J.; Rebesco, M.; Porter, M.E.; Nicastro, D. Cryoelectron tomography reveals doublet-specific structures and unique interactions in the II dynein. *Proc. Natl. Acad. Sci. USA* **2012**, *109*, E2067–E2076. [[CrossRef](#)] [[PubMed](#)]
34. Dymek, E.E.; Heuser, T.; Nicastro, D.; Smith, E.F. The CSC is required for complete radial spoke assembly and wild-type ciliary motility. *Mol. Biol. Cell* **2011**, *22*, 2520–2531. [[CrossRef](#)] [[PubMed](#)]
35. Heuser, T.; Dymek, E.E.; Lin, J.; Smith, E.F.; Nicastro, D. The CSC connects three major axonemal complexes involved in dynein regulation. *Mol. Biol. Cell* **2012**, *23*, 3143–3155. [[CrossRef](#)] [[PubMed](#)]
36. Yamamoto, R.; Song, K.; Yanagisawa, H.A.; Fox, L.; Yagi, T.; Wirschell, M.; Hirono, M.; Kamiya, R.; Nicastro, D.; Sale, W.S. The MIA complex is a conserved and novel dynein regulator essential for normal ciliary motility. *J. Cell Biol.* **2013**, *201*, 263–278. [[CrossRef](#)] [[PubMed](#)]
37. Bazan, R.; Schröfel, A.; Joachimiak, E.; Poprzeczko, M.; Pigino, G.; Włoga, D. Ccdc113/Ccdc96 complex, a novel regulator of ciliary beating that connects radial spoke 3 to dynein g and the nexin link. *PLoS Genet.* **2021**, *17*, e1009388. [[CrossRef](#)]
38. Samsel, Z.; Sekretarska, J.; Osinka, A.; Włoga, D.; Joachimiak, E. Central apparatus, the molecular kickstarter of ciliary and flagellar nanomachines. *Int. J. Mol. Sci.* **2021**, *22*, 3013. [[CrossRef](#)]
39. Sun, S.; Fisher, R.L.; Bowser, S.S.; Pentecost, B.T.; Sui, H. Three-dimensional architecture of epithelial primary cilia. *Proc. Natl. Acad. Sci. USA* **2019**, *116*, 9370–9379. [[CrossRef](#)]
40. Flock, A.; Duvall, A.J. The ultrastructure of the kinocilium of the sensory cells in the inner ear and lateral line organs. *J. Cell Biol.* **1965**, *25*, 1–8. [[CrossRef](#)]

41. Sobkowicz, H.M.; Slapnick, S.M.; August, B.K. The kinocilium of auditory hair cells and evidence for its morphogenetic role during the regeneration of stereocilia and cuticular plates. *J. Neurocytol.* **1995**, *24*, 633–653. [CrossRef] [PubMed]
42. Kikuchi, T.; Takasaka, T.; Tonosaki, A.; Watanabe, H. Fine structure of Guinea pig vestibular kinocilium. *Acta Otolaryngol.* **1989**, *108*, 26–30. [CrossRef] [PubMed]
43. Shah, A.S.; Yehuda, B.S.; Moninger, T.O.; Kline, J.N.; Welsh, M.J. Motile cilia of human airway epithelia are chemosensory. *Science* **2009**, *325*, 1131–1134. [CrossRef] [PubMed]
44. Jain, R.; Javidan-Nejad, C.; Alexander-Brett, J.; Horani, A.; Cabellon, M.C.; Walter, M.J.; Brody, S.L. Sensory functions of motile cilia and implication for bronchiectasis. *Front. Biosci.-Sch.* **2012**, *4*, 1088–1098. [CrossRef]
45. Mitchison, H.M.; Valente, E.M. Motile and non-motile cilia in human pathology: From function to phenotypes. *J. Pathol.* **2017**, *241*, 294–309. [CrossRef]
46. Ringers, C.; Olstad, E.W.; Jurisch-Yaksi, N. The role of motile cilia in the development and physiology of the nervous system. *Philos. Trans. R. Soc. B Biol. Sci.* **2019**, *375*, 20190156. [CrossRef]
47. Legendre, M.; Zaragoza, L.E.; Mitchison, H.M. Motile cilia and airway disease. *Semin. Cell Dev. Biol.* **2020**, *110*, 19–33. [CrossRef]
48. Bustamante-Marin, X.M.; Yin, W.N.; Sears, P.R.; Werner, M.E.; Brotslaw, E.J.; Mitchell, B.J.; Jania, C.M.; Zeman, K.L.; Rogers, T.D.; Herring, L.E.; et al. Lack of GAS2L2 Causes PCD by Impairing Cilia Orientation and Mucociliary Clearance. *Am. J. Hum. Genet.* **2019**, *104*, 229–245. [CrossRef]
49. Little, R.B.; Norris, D.P. Right, left and cilia: How asymmetry is established. *Semin. Cell Dev. Biol.* **2021**, *110*, 11–18. [CrossRef]
50. Brennan, S.K.; Ferkol, T.W.; Davis, S.D. Emerging genotype-phenotype relationships in primary ciliary dyskinesia. *Int. J. Mol. Sci.* **2021**, *22*, 8272. [CrossRef]
51. Focsa, I.O.; Budisteanu, M.; Bălgrădean, M. Clinical and genetic heterogeneity of primary ciliopathies (Review). *Int. J. Mol. Med.* **2021**, *48*, 176. [CrossRef] [PubMed]
52. Tobin, J.L.; Beales, P.L. The nonmotile ciliopathies. *Genet. Med.* **2009**, *11*, 386–402. [CrossRef]
53. Horani, A.; Ferkol, T.W. Advances in the Genetics of Primary Ciliary Dyskinesia: Clinical Implications. *Chest* **2018**, *154*, 645–652. [CrossRef] [PubMed]
54. Antony, D.; Brunner, H.G.; Schmidts, M. Ciliary dyneins and dynein related ciliopathies. *Cells* **2021**, *10*, 1885. [CrossRef] [PubMed]
55. Poprzeczko, M.; Bicka, M.; Farahat, H.; Bazan, R.; Osinka, A.; Fabczak, H.; Joachimiak, E.; Włoga, D. Rare Human Diseases: Model Organisms in Deciphering the Molecular Basis of Primary Ciliary Dyskinesia. *Cells* **2019**, *8*, 1614. [CrossRef] [PubMed]
56. Lewis, M.; Stracker, T.H. Transcriptional regulation of multiciliated cell differentiation. *Semin. Cell Dev. Biol.* **2021**, *110*, 51–60. [CrossRef]
57. Carvalho-Santos, Z.; Azimzadeh, J.; Pereira-Leal, J.B.; Bettencourt-Dias, M. Tracing the origins of centrioles, cilia, and flagella. *J. Cell Biol.* **2011**, *194*, 165–175. [CrossRef]
58. Khan, S.; Scholey, J.M. Assembly, Functions and Evolution of Archaela, Flagella and Cilia. *Curr. Biol.* **2018**, *28*, R278–R292. [CrossRef]
59. Mitchell, D.R. Evolution of cilia. *Cold Spring Harb. Perspect. Biol.* **2017**, *9*, 1–12. [CrossRef]
60. Horani, A.; Ferkol, T.W. Primary ciliary dyskinesia and associated sensory ciliopathies. *Expert Rev. Respir. Med.* **2016**, *10*, 569–576. [CrossRef]
61. Brndiarova, M.; Kvassayova, J.; Vojtkova, J.; Igaz, M.; Buday, T.; Plevkova, J. Changes of Motile Ciliary Phenotype in Patients with Primary Ciliopathies. *Adv. Exp. Med. Biol.* **2021**, *1335*, 79–85.
62. Kempeneers, C.; Chilvers, M.A. To beat, or not to beat, that is question! The spectrum of ciliopathies. *Pediatr. Pulmonol.* **2018**, *53*, 1122–1129. [CrossRef]
63. Vertii, A.; Bright, A.; Delaval, B.; Hehnly, H.; Doxsey, S. New frontiers: Discovering cilia-independent functions of cilia proteins. *EMBO Rep.* **2015**, *16*, 1275–1287. [CrossRef] [PubMed]
64. Russell, W.M.S.; Burch, R.L. *The Principles of Humane Experimental Technique*; Universities Federation for Animal Welfare: Hertfordshire, UK, 1959; ISBN 0-900767-78-2.
65. Pazour, G.J.; Agrin, N.; Leszyk, J.; Witman, G.B. Proteomic analysis of a eukaryotic cilium. *J. Cell Biol.* **2005**, *170*, 103–113. [CrossRef] [PubMed]
66. Smith, J.C.; Northe, J.G.B.; Garg, J.; Pearlman, R.E.; Siu, K.W.M. Robust method for proteome analysis by MS/MS using an entire translated genome: Demonstration on the ciliome of Tetrahymena thermophila. *J. Proteome Res.* **2005**, *4*, 909–919. [CrossRef] [PubMed]
67. Subota, I.; Julkowska, D.; Vincensini, L.; Reeg, N.; Buisson, J.; Blisnick, T.; Huet, D.; Perrot, S.; Santi-Rocca, J.; Duchateau, M.; et al. Proteomic analysis of intact flagella of procyclic Trypanosoma brucei cells identifies novel flagellar proteins with unique sub-localization and dynamics. *Mol. Cell. Proteomics* **2014**, *13*, 1769–1786. [CrossRef]
68. Pigino, G.; Bui, K.H.; Maheshwari, A.; Lupetti, P.; Diener, D.; Ishikawa, T. Cryoelectron tomography of radial spokes in cilia and flagella. *J. Cell Biol.* **2011**, *195*, 673–687. [CrossRef]
69. Barber, C.F.; Heuser, T.; Carbajal-González, B.I.; Botchkarev, V.V.; Nicastro, D. Three-dimensional structure of the radial spokes reveals heterogeneity and interactions with dyneins in Chlamydomonas flagella. *Mol. Biol. Cell* **2012**, *23*, 111–120. [CrossRef]
70. Tuxhorn, J.; Daise, T.; Dentler, W.L. Regulation of Flagellar Length in Chlamydomonas. *Cytoskeleton* **1998**, *40*, 133–146. [CrossRef]
71. Salomé, P.A.; Merchant, S.S. A series of fortunate events: Introducing chlamydomonas as a reference organism. *Plant Cell* **2019**, *31*, 1682–1707. [CrossRef]

72. Harris, E.H. Chlamydomonas as a model organism. *Annu. Rev. Plant Biol.* **2001**, *52*, 363–406. [CrossRef] [PubMed]
73. Jinkerson, R.E.; Jonikas, M.C. Molecular techniques to interrogate and edit the Chlamydomonas nuclear genome. *Plant J.* **2015**, *82*, 393–412. [CrossRef] [PubMed]
74. Lin, H.; Dutcher, S.K. Genetic and genomic approaches to identify genes involved in flagellar assembly in Chlamydomonas reinhardtii. *Methods Cell Biol.* **2015**, *127*, 349–386. [CrossRef] [PubMed]
75. Harris, E.H. Chlamydomonas in the laboratory. In *The Chlamydomonas Sourcebook: Introduction to Chlamydomonas and Its Laboratory Use*; Elsevier Academic Press: Amsterdam, The Netherlands, 2008; pp. 241–302. ISBN 9780123708748.
76. Li, X.; Zhang, R.; Patena, W.; Gang, S.S.; Blum, S.R.; Ivanova, N.; Yue, R.; Robertson, J.M.; Lefebvre, P.A.; Fitz-Gibbon, S.T.; et al. An Indexed, Mapped Mutant Library Enables Reverse Genetics Studies of Biological Processes in Chlamydomonas reinhardtii. *Plant Cell* **2016**, *28*, 367–387. [CrossRef]
77. Li, X.; Patena, W.; Fauser, F.; Jinkerson, R.E.; Saroussi, S.; Meyer, M.T.; Ivanova, N.; Robertson, J.M.; Yue, R.; Zhang, R.; et al. A genome-wide algal mutant library and functional screen identifies genes required for eukaryotic photosynthesis. *Nat. Genet.* **2019**, *51*, 627–635. [CrossRef]
78. Dhokane, D.; Bhadra, B.; Dasgupta, S. CRISPR based targeted genome editing of Chlamydomonas reinhardtii using programmed Cas9-gRNA ribonucleoprotein. *Mol. Biol. Rep.* **2020**, *47*, 8747–8755. [CrossRef]
79. Shin, S.E.; Lim, J.M.; Koh, H.G.; Kim, E.K.; Kang, N.K.; Jeon, S.; Kwon, S.; Shin, W.S.; Lee, B.; Hwangbo, K.; et al. CRISPR/Cas9-induced knockout and knock-in mutations in Chlamydomonas reinhardtii. *Sci. Rep.* **2016**, *6*, 27810. [CrossRef]
80. Guzmán-Zapata, D.; Sandoval-Vargas, J.M.; Macedo-Osorio, K.S.; Salgado-Manjarrez, E.; Castrejón-Flores, J.L.; Oliver-Salvador, M.D.C.; Durán-Figueroa, N.V.; Nogué, F.; Badillo-Corona, J.A. Efficient editing of the nuclear APT reporter gene in chlamydomonas reinhardtii via expression of a CRISPR-Cas9 module. *Int. J. Mol. Sci.* **2019**, *20*, 1247. [CrossRef]
81. Picariello, T.; Hou, Y.; Kubo, T.; McNeill, N.A.; Yanagisawa, H.A.; Oda, T.; Witman, G.B. TIM, a targeted insertional mutagenesis method utilizing CRISPR/Cas9 in Chlamydomonas reinhardtii. *PLoS ONE* **2020**, *15*, e0232594. [CrossRef]
82. Kindle, K.L. High-frequency nuclear transformation of Chlamydomonas reinhardtii. *Proc. Natl. Acad. Sci. USA* **1990**, *87*, 1228–1232. [CrossRef]
83. Shimogawara, K.; Fujiwara, S.; Grossman, A.; Usuda, H. High-efficiency transformation of Chlamydomonas reinhardtii by electroporation. *Genetics* **1998**, *148*, 1821–1828. [CrossRef] [PubMed]
84. Kindle, K.L.; Schnell, R.A.; Fernandez, E.; Lefebvre, P.A. Stable nuclear transformation of Chlamydomonas using the Chlamydomonas gene for nitrate reductase. *J. Cell Biol.* **1989**, *109*, 2589–2601. [CrossRef] [PubMed]
85. Kumar, S.V.; Misquitta, R.W.; Reddy, V.S.; Rao, B.J.; Rajam, M.V. Genetic transformation of the green alga - Chlamydomonas reinhardtii by Agrobacterium tumefaciens. *Plant Sci.* **2004**, *166*, 731–738. [CrossRef]
86. Park, R.V.; Asbury, H.; Miller, S.M. Modification of a Chlamydomonas reinhardtii CRISPR/Cas9 transformation protocol for use with widely available electroporation equipment. *MethodsX* **2020**, *7*, 100855. [CrossRef] [PubMed]
87. Kang, S.; Jeon, S.; Kim, S.; Chang, Y.K.; Kim, Y.C. Development of a pVEC peptide-based ribonucleoprotein (RNP) delivery system for genome editing using CRISPR/Cas9 in Chlamydomonas reinhardtii. *Sci. Rep.* **2020**, *10*, 22158. [CrossRef]
88. Wakabayashi, K.I.; Kamiya, R. Axonemal motility in Chlamydomonas. *Methods Cell Biol.* **2015**, *127*, 387–402. [CrossRef]
89. Oda, T.; Yanagisawa, H.; Kamiya, R.; Kikkawa, M. A molecular ruler determines the repeat length in eukaryotic cilia and flagella. *Science* **2014**, *346*, 857–860. [CrossRef]
90. King, S.M.; Patel-King, R.S. The oligomeric outer dynein arm assembly factor CCDC103 is tightly integrated within the cilial axoneme and exhibits periodic binding to microtubules. *J. Biol. Chem.* **2015**, *290*, 7388–7401. [CrossRef]
91. Panizzi, J.R.; Becker-Heck, A.; Castleman, V.H.; Al-Mutairi, D.A.; Liu, Y.; Loges, N.T.; Pathak, N.; Austin-Tse, C.; Sheridan, E.; Schmidts, M.; et al. CCDC103 mutations cause primary ciliary dyskinesia by disrupting assembly of cilial dynein arms. *Nat. Genet.* **2012**, *44*, 714–719. [CrossRef]
92. Heuser, T.; Raytchev, M.; Krell, J.; Porter, M.E.; Nicastro, D. The dynein regulatory complex is the nexin link and a major regulatory node in cilia and flagella. *J. Cell Biol.* **2009**, *187*, 921–933. [CrossRef]
93. Yang, P.; Diener, D.R.; Yang, C.; Kohno, T.; Pazour, G.J.; Dienes, J.M.; Agrin, N.S.; King, S.M.; Sale, W.S.; Kamiya, R.; et al. Radial spoke proteins of Chlamydomonas flagella. *J. Cell Sci.* **2006**, *119*, 1165–1174. [CrossRef]
94. Castleman, V.H.; Romio, L.; Chodhari, R.; Hirst, R.A.; de Castro, S.C.P.; Parker, K.A.; Ybot-Gonzalez, P.; Emes, R.D.; Wilson, S.W.; Wallis, C.; et al. Mutations in radial spoke head protein genes RSPH9 and RSPH4A cause primary ciliary dyskinesia with central-microtubular-pair abnormalities. *Am. J. Hum. Genet.* **2008**, *84*, 197–209. [CrossRef] [PubMed]
95. Williams, B.D.; Velleca, M.A.; Curry, A.M.; Rosenbaum, J.L. Molecular cloning and sequence analysis of the Chlamydomonas gene coding for radial spoke protein 3: Flagellar mutation pf-14 is an ochre allele. *J. Cell Biol.* **1989**, *109*, 235–245. [CrossRef]
96. Bustamante-Marin, X.M.; Horani, A.; Stoyanova, M.; Charny, W.L.; Bottier, M.; Sears, P.R.; Yin, W.N.; Daniels, L.A.; Bowen, H.; Conrad, D.F.; et al. Mutation of CFAP57, a protein required for the asymmetric targeting of a subset of inner dynein arms in Chlamydomonas, causes primary ciliary dyskinesia. *PLoS Genet.* **2020**, *16*, e1008691. [CrossRef] [PubMed]
97. Lin, J.; Le, T.V.; Augspurger, K.; Tritschler, D.; Bower, R.; Fu, G.; Perrone, C.; O’Toole, E.T.; Mills, K.V.; Dymek, E.; et al. FAP57/WDR65 targets assembly of a subset of inner arm dyneins and connects to regulatory hubs in cilia. *Mol. Biol. Cell* **2019**, *30*, 2659–2680. [CrossRef]
98. Zhang, H.; Mitchell, D.R. Cpc1, a Chlamydomonas central pair protein with an adenylate kinase domain. *J. Cell Sci.* **2004**, *117*, 4179–4188. [CrossRef] [PubMed]

99. DiPetrillo, C.G.; Smith, E.F. Pcdp1 is a central apparatus protein that binds  $\text{Ca}^{2+}$ -calmodulin and regulates ciliary motility. *J. Cell Biol.* **2010**, *189*, 601–612. [CrossRef]
100. Lechtreck, K.F.; Witman, G.B. Chlamydomonas reinhardtii hydin is a central pair protein required for flagellar motility. *J. Cell Biol.* **2007**, *176*, 473–482. [CrossRef]
101. Smith, E.F.; Lefebvre, P.A. PF16 encodes a protein with armadillo repeats and localizes to a single microtubule of the central apparatus in Chlamydomonas flagella. *J. Cell Biol.* **1996**, *132*, 359–370. [CrossRef] [PubMed]
102. Fu, G.; Zhao, L.; Dymek, E.; Hou, Y.; Song, K.; Phan, N.; Shang, Z.; Smith, E.F.; Witman, G.B.; Nicastro, D. Structural organization of the C1a-e-c supercomplex within the ciliary central apparatus. *J. Cell Biol.* **2019**, *218*, 4236–4251. [CrossRef] [PubMed]
103. Wu, H.; Wang, J.; Cheng, H.; Gao, Y.; Liu, W.; Zhang, Z.; Jiang, H.; Li, W.; Zhu, F.; Lv, M.; et al. Patients with severe asthenoteratospermia carrying SPAG6 or RSPH3 mutations have a positive pregnancy outcome following intracytoplasmic sperm injection. *J. Assist. Reprod. Genet.* **2020**, *37*, 829–840. [CrossRef] [PubMed]
104. Rupp, G.; O’Toole, E.; Gardner, L.C.; Mitchell, B.F.; Porter, M.E. The sup-pf-2 mutations of Chlamydomonas alter the activity of the outer dynein arms by modification of the gamma-dynein heavy chain. *J. Cell Biol.* **1996**, *135*, 1853–1865. [CrossRef]
105. Wilkerson, C.G.; King, S.M.; Koutoulis, A.; Pazour, G.J.; Witman, G.B. The 78,000 M(r) intermediate chain of Chlamydomonas outer arm dynein is a WD-repeat protein required for arm assembly. *J. Cell Biol.* **1995**, *129*, 169–178. [CrossRef]
106. Mitchell, D.R.; Kang, Y. Reversion analysis of dynein intermediate chain function. *J. Cell Sci.* **1993**, *105*, 1069–1078. [CrossRef]
107. Pennarun, G.; Escudier, E.; Chapelin, C.; Bridoux, A.M.; Cacheux, V.; Roger, G.; Clément, A.; Goossens, M.; Amselem, S.; Duriez, B. Loss-of-function mutations in a human gene related to Chlamydomonas reinhardtii dynein IC78 result in primary ciliary dyskinesia. *Am. J. Hum. Genet.* **1999**, *65*, 1508–1519. [CrossRef]
108. Olbrich, H.; Häffner, K.; Kispert, A.; Völkel, A.; Volz, A.; Sasmaz, G.; Reinhardt, R.; Hennig, S.; Lehrach, H.; Konietzko, N.; et al. Mutations in DNAH5 cause primary ciliary dyskinesia and randomization of left-right asymmetry. *Nat. Genet.* **2002**, *30*, 143–144. [CrossRef]
109. Loges, N.T.; Olbrich, H.; Fenske, L.; Mussaffi, H.; Horvath, J.; Fliegauf, M.; Kuhl, H.; Baktai, G.; Peterffy, E.; Chodhari, R.; et al. DNAI2 mutations cause primary ciliary dyskinesia with defects in the outer dynein arm. *Am. J. Hum. Genet.* **2008**, *83*, 547–558. [CrossRef] [PubMed]
110. Leigh, M.W.; Pittman, J.E.; Carson, J.L.; Ferkol, T.W.; Dell, S.D.; Davis, S.D.; Knowles, M.R.; Zariwala, M.A. Clinical and genetic aspects of primary ciliary dyskinesia/kartagener syndrome. *Genet. Med.* **2009**, *11*, 473–487. [CrossRef] [PubMed]
111. Austin-Tse, C.; Halbritter, J.; Zariwala, M.A.; Gilberti, R.M.; Gee, H.Y.; Hellman, N.; Pathak, N.; Liu, Y.; Panizzi, J.R.; Patel-King, R.S.; et al. Zebrafish ciliopathy screen plus human mutational analysis identifies C21orf59 and CCDC65 defects as causing primary ciliary dyskinesia. *Am. J. Hum. Genet.* **2013**, *93*, 672–686. [CrossRef]
112. Fassad, M.R.; Shoemark, A.; le Borgne, P.; Koll, F.; Patel, M.; Dixon, M.; Hayward, J.; Richardson, C.; Frost, E.; Jenkins, L.; et al. C21orf70 Mutations Disrupting the Intraflagellar Transport-Dependent Assembly of Multiple Axonemal Dyneins Cause Primary Ciliary Dyskinesia. *Am. J. Hum. Genet.* **2018**, *102*, 956–972. [CrossRef] [PubMed]
113. Duquesnoy, P.; Escudier, E.; Vincensini, L.; Freshour, J.; Bridoux, A.M.; Coste, A.; Deschildre, A.; de Blic, J.; Legendre, M.; Montantin, G.; et al. Loss-of-Function Mutations in the Human Ortholog of Chlamydomonas reinhardtii ODA7 Disrupt Dynein Arm Assembly and Cause Primary Ciliary Dyskinesia. *Am. J. Hum. Genet.* **2009**, *85*, 890–896. [CrossRef] [PubMed]
114. Kamiya, R. Mutations at twelve independent loci result in absence of outer dynein arms in Chlamydomonas reinhardtii. *J. Cell Biol.* **1988**, *107*, 2253–2258. [CrossRef] [PubMed]
115. Freshour, J.; Yokoyama, R.; Mitchell, D.R. Chlamydomonas flagellar outer row dynein assembly protein ODA7 interacts with both outer row and I1 inner row dyneins. *J. Biol. Chem.* **2007**, *282*, 5404–5412. [CrossRef] [PubMed]
116. Huang, B.; Piperno, G.; Luck, D.J.L. Paralyzed flagella mutants of Chlamydomonas reinhardtii. Defective for axonemal doublet microtubule arms. *J. Biol. Chem.* **1979**, *254*, 3091–3099. [CrossRef]
117. Omran, H.; Kobayashi, D.; Olbrich, H.; Tsukahara, T.; Loges, N.T.; Hagiwara, H.; Zhang, Q.; Leblond, G.; O’Toole, E.; Hara, C.; et al. Ktu/PF13 is required for cytoplasmic pre-assembly of axonemal dyneins. *Nature* **2008**, *456*, 611–616. [CrossRef] [PubMed]
118. Yamamoto, R.; Yanagi, S.; Nagao, M.; Yamasaki, Y.; Tanaka, Y.; Sale, W.S.; Yagi, T.; Kon, T. Mutations in PIH proteins MOT48, TWI1 and PF13 define common and unique steps for preassembly of each, different ciliary dynein. *PLoS Genet.* **2020**, *16*, e1009126. [CrossRef]
119. Mitchison, H.M.; Schmidts, M.; Loges, N.T.; Freshour, J.; Dritsoula, A.; Hirst, R.A.; O’Callaghan, C.; Blau, H.; Al Dabbagh, M.; Olbrich, H.; et al. Mutations in axonemal dynein assembly factor DNAAF3 cause primary ciliary dyskinesia. *Nat. Genet.* **2012**, *44*, 381–389. [CrossRef]
120. Yamamoto, R.; Obbineni, J.M.; Alford, L.M.; Ide, T.; Owa, M.; Hwang, J.; Kon, T.; Inaba, K.; James, N.; King, S.M.; et al. Chlamydomonas DYX1C1/PF23 is essential for axonemal assembly and proper morphology of inner dynein arms. *PLoS Genet.* **2017**, *13*, e1006996. [CrossRef]
121. Horani, A.; Druley, T.E.; Zariwala, M.A.; Patel, A.C.; Levinson, B.T.; Van Arendonk, L.G.; Thornton, K.C.; Giacalone, J.C.; Albee, A.J.; Wilson, K.S.; et al. Whole-exome capture and sequencing identifies HEATR2 mutation as a cause of primary ciliary dyskinesia. *Am. J. Hum. Genet.* **2012**, *91*, 685–693. [CrossRef]
122. Yamamoto, R.; Hirono, M.; Kamiya, R. Discrete PIH proteins function in the cytoplasmic preassembly of different subsets of axonemal dyneins. *J. Cell Biol.* **2010**, *190*, 65–71. [CrossRef]

123. Desai, P.B.; Freshour, J.R.; Mitchell, D.R. Chlamydomonas axonemal dynein assembly locus ODA8 encodes a conserved flagellar protein needed for cytoplasmic maturation of outer dynein arm complexes. *Cytoskeleton* **2015**, *72*, 16–28. [CrossRef]
124. Fabczak, H.; Osinka, A. Role of the novel Hsp90 co-chaperones in dynein arms' preassembly. *Int. J. Mol. Sci.* **2019**, *20*, 6174. [CrossRef] [PubMed]
125. Owa, M.; Uchihashi, T.; aki Yanagisawa, H.; Yamano, T.; Iguchi, H.; Fukuzawa, H.; ichi Wakabayashi, K.; Ando, T.; Kikkawa, M. Inner lumen proteins stabilize doublet microtubules in cilia and flagella. *Nat. Commun.* **2019**, *10*, 1–12. [CrossRef] [PubMed]
126. Vasudevan, K.K.; Song, K.; Alford, L.M.; Sale, W.S.; Dymek, E.E.; Smith, E.F.; Hennessey, T.; Joachimiak, E.; Urbanska, P.; Wloga, D.; et al. FAP206 is a microtubule-docking adapter for ciliary radial spoke 2 and dynein c. *Mol. Biol. Cell* **2015**, *26*, 696–710. [CrossRef] [PubMed]
127. Fu, G.; Wang, Q.; Phan, N.; Urbanska, P.; Joachimiak, E.; Lin, J.; Wloga, D.; Nicastro, D. The I1 dynein-associated tether and tether head complex is a conserved regulator of ciliary motility. *Mol. Biol. Cell* **2018**, *29*, 1048–1059. [CrossRef] [PubMed]
128. Rotureau, B.; Subota, I.; Bastin, P. Molecular bases of cytoskeleton plasticity during the Trypanosoma brucei parasite cycle. *Cell. Microbiol.* **2011**, *13*, 705–716. [CrossRef]
129. Bertiaux, E.; Mallet, A.; Rotureau, B.; Bastin, P. Intraflagellar transport during assembly of flagella of different length in Trypanosoma brucei isolated from tsetse flies. *J. Cell Sci.* **2020**, *133*, jcs248989. [CrossRef]
130. An, T.; Zhou, Q.; Hu, H.; Cormaty, H.; Li, Z. FAZ27 cooperates with FLAM3 and ClpGM6 to maintain cell morphology in Trypanosoma brucei. *J. Cell Sci.* **2020**, *133*, jcs245258. [CrossRef]
131. Langousis, G.; Hill, K.L. Motility and more: The flagellum of Trypanosoma brucei. *Nat. Rev. Microbiol.* **2014**, *12*, 505–518. [CrossRef]
132. Oberholzer, M.; Lopez, M.A.; Ralston, K.S.; Hill, K.L. Approaches for functional analysis of flagellar proteins in African trypanosomes. *Methods Cell Biol.* **2009**, *93*, 21–57. [CrossRef]
133. Wirtz, E.; Leal, S.; Ochatt, C.; Cross, G.M. A tightly regulated inducible expression system for conditional gene knock-outs and dominant-negative genetics in Trypanosoma brucei. *Mol. Biochem. Parasitol.* **1999**, *99*, 89–101. [CrossRef]
134. Santi-Rocca, J.; Chenouard, N.; Fort, C.; Lagache, T.; Olivo-Marin, J.C.; Bastin, P. Imaging intraflagellar transport in trypanosomes. *Methods Cell Biol.* **2015**, *127*, 487–508. [CrossRef] [PubMed]
135. Burkard, G.; Fragoso, C.M.; Roditi, I. Highly efficient stable transformation of bloodstream forms of Trypanosoma brucei. *Mol. Biochem. Parasitol.* **2007**, *153*, 220–223. [CrossRef] [PubMed]
136. MacGregor, P.; Rojas, F.; Dean, S.; Matthews, K.R. Stable transformation of pleomorphic bloodstream form Trypanosoma brucei. *Mol. Biochem. Parasitol.* **2013**, *190*, 60–62. [CrossRef] [PubMed]
137. Bachmaier, S.; Thanner, T.; Boshart, M. Culturing and Transfection of Pleomorphic Trypanosoma brucei. *Methods Mol. Biol.* **2020**, *2116*, 23–38. [PubMed]
138. Yagoubat, A.; Corrales, R.M.; Bastien, P.; Lévéque, M.F.; Sterkers, Y. Gene Editing in Trypanosomatids: Tips and Tricks in the CRISPR-Cas9 Era. *Trends Parasitol.* **2020**, *36*, 745–760. [CrossRef]
139. Medeiros, L.C.S.; South, L.; Peng, D.; Bustamante, J.M.; Wang, W.; Bunkofske, M.; Perumal, N.; Sanchez-Valdez, F.; Tarleton, R.L. Rapid, selection-free, high-efficiency genome editing in protozoan parasites using CRISPR-cas9 ribonucleoproteins. *MBio* **2017**, *8*, e01788-17. [CrossRef]
140. Lander, N.; Chiurillo, M.A. State-of-the-art CRISPR/Cas9 Technology for Genome Editing in Trypanosomatids. *J. Eukaryot. Microbiol.* **2019**, *66*, 981–991. [CrossRef]
141. Baron, D.M.; Kabututu, Z.P.; Hill, K.L. Stuck in reverse: Loss of LC1 in Trypanosoma brucei disrupts outer dynein arms and leads to reverse flagellar beat and backward movement. *J. Cell Sci.* **2007**, *120*, 1513–1520. [CrossRef]
142. Ralston, K.S.; Lerner, A.G.; Diener, D.R.; Hill, K.L. Flagellar motility contributes to cytokinesis in Trypanosoma brucei and is modulated by an evolutionarily conserved dynein regulatory system. *Eukaryot. Cell* **2006**, *5*, 696–711. [CrossRef]
143. Branche, C.; Kohl, L.; Toutirais, G.; Buisson, J.; Cosson, J.; Bastin, P. Conserved and specific functions of axoneme components in trypanosome motility. *J. Cell Sci.* **2006**, *119*, 3443–3455. [CrossRef] [PubMed]
144. Krüger, T.; Engstler, M. Motility Analysis of Trypanosomatids. *Methods Mol. Biol.* **2020**, *2116*, 409–423. [PubMed]
145. Höög, J.L.; Bouchet-Marquis, C.; McIntosh, J.R.; Hoenger, A.; Gull, K. Cryo-electron tomography and 3-D analysis of the intact flagellum in Trypanosoma brucei. *J. Struct. Biol.* **2012**, *178*, 189–198. [CrossRef] [PubMed]
146. Imhof, S.; Zhang, J.; Wang, H.; Bui, K.H.; Nguyen, H.; Atanasov, I.; Hui, W.H.; Yang, S.K.; Zhou, Z.H.; Hill, K.L. Cryo-electron tomography with volta phase plate reveals novel structural foundations of the 96-nm axonemal repeat in the pathogen trypanosoma brucei. *Elife* **2019**, *8*, e52058. [CrossRef]
147. Motta, M.C.M.; Catta-Preta, C.M.C. Electron Microscopy Techniques Applied to Symbiont-Harboring Trypanosomatids: The Association of the Bacterium with Host Organelles. *Methods Mol. Biol.* **2020**, *2116*, 425–447.
148. Kabututu, Z.P.; Thayer, M.; Melehani, J.H.; Hill, K.L. CMF70 is a subunit of the dynein regulatory complex. *J. Cell Sci.* **2010**, *123*, 3587–3595. [CrossRef]
149. Hutchings, N.R.; Donelson, J.E.; Hill, K.L. Trypanin is a cytoskeletal linker protein and is required for cell motility in African trypanosomes. *J. Cell Biol.* **2002**, *156*, 867–877. [CrossRef]
150. Dawe, H.R.; Shaw, M.K.; Farr, H.; Gull, K. The hydrocephalus inducing gene product, Hydin, positions axonemal central pair microtubules. *BMC Biol.* **2007**, *5*, 1–10. [CrossRef]

151. Bonnefoy, S.; Watson, C.M.; Kernohan, K.D.; Lemos, M.; Hutchinson, S.; Poulter, J.A.; Crinnion, L.A.; Berry, I.; Simmonds, J.; Vasudevan, P.; et al. Biallelic Mutations in LRRC56, Encoding a Protein Associated with Intraflagellar Transport, Cause Mucociliary Clearance and Laterality Defects. *Am. J. Hum. Genet.* **2018**, *103*, 727–739. [CrossRef]
152. Aprea, I.; Raidt, J.; Höben, I.M.; Loges, N.T.; Nöthe-Menchen, T.; Pennekamp, P.; Olbrich, H.; Kaiser, T.; Biebach, L.; Tüttelmann, F.; et al. Defects in the cytoplasmic assembly of axonemal dynein arms cause morphological abnormalities and dysmotility in sperm cells leading to male infertility. *PLoS Genet.* **2021**, *17*, e1009306. [CrossRef]
153. Kott, E.; Duquesnoy, P.; Copin, B.; Legendre, M.; Dastot-Le Moal, F.; Montantin, G.; Jeanson, L.; Tamalet, A.; Papon, J.F.; Siffroi, J.P.; et al. Loss-of-function mutations in LRRC6, a gene essential for proper axonemal assembly of inner and outer dynein arms, cause primary ciliary dyskinesia. *Am. J. Hum. Genet.* **2012**, *91*, 958–964. [CrossRef] [PubMed]
154. Morgan, G.W.; Denny, P.W.; Vaughan, S.; Goulding, D.; Jeffries, T.R.; Smith, D.F.; Gull, K.; Field, M.C. An Evolutionarily Conserved Coiled-Coil Protein Implicated in Polycystic Kidney Disease Is Involved in Basal Body Duplication and Flagellar Biogenesis in *Trypanosoma brucei*. *Mol. Cell. Biol.* **2005**, *25*, 3774–3783. [CrossRef] [PubMed]
155. Coutton, C.; Vargas, A.S.; Amiri-Yekta, A.; Kherraf, Z.E.; Mustapha, S.F.B.; Le Tanno, P.; Wambergue-Legrand, C.; Karaouzène, T.; Martinez, G.; Crouzy, S.; et al. Mutations in CFAP43 and CFAP44 cause male infertility and flagellum defects in *Trypanosoma* and human. *Nat. Commun.* **2018**, *9*, 686. [CrossRef] [PubMed]
156. Martinez, G.; Beurois, J.; Dacheux, D.; Cazin, C.; Bidart, M.; Kherraf, Z.E.; Robinson, D.R.; Satre, V.; Le Gac, G.; Ka, C.; et al. Biallelic variants in MAATS1 encoding CFAP91, a calmodulin-associated and spoke-associated complex protein, cause severe astheno-teratozoospermia and male infertility. *J. Med. Genet.* **2020**, *57*, 708–716. [CrossRef]
157. Kherraf, Z.E.; Amiri-Yekta, A.; Dacheux, D.; Karaouzène, T.; Coutton, C.; Christou-Kent, M.; Martinez, G.; Landrein, N.; Le Tanno, P.; Mustapha, S.F.B.; et al. A Homozygous Ancestral SVA-Insertion-Mediated Deletion in WDR66 Induces Multiple Morphological Abnormalities of the Sperm Flagellum and Male Infertility. *Am. J. Hum. Genet.* **2018**, *103*, 400–412. [CrossRef]
158. Lorès, P.; Dacheux, D.; Kherraf, Z.E.; Mbango, J.F.N.; Coutton, C.; Stouvenel, L.; Italy-Radio, C.; Amiri-Yekta, A.; Whitfield, M.; Schmitt, A.; et al. Mutations in TTC29, Encoding an Evolutionarily Conserved Axonemal Protein, Result in Asthenozoospermia and Male Infertility. *Am. J. Hum. Genet.* **2019**, *105*, 1148–1167. [CrossRef]
159. Lynn, D. Ciliates. *Encycl. Microbiol.* **2009**, 578–592.
160. Wloga, D.; Frankel, J. From Molecules to Morphology: Cellular Organization of *Tetrahymena thermophila*. *Methods Cell Biol.* **2012**, *109*, 83–140.
161. Aubusson-Fleury, A.; Cohen, J.; Lemullois, M. Ciliary heterogeneity within a single cell: The Paramecium model. *Methods Cell Biol.* **2015**, *127*, 457–485.
162. Tassin, A.M.; Lemullois, M.; Aubusson-Fleury, A. Paramecium tetraurelia basal body structure. *Cilia* **2016**, *5*. [CrossRef]
163. Valentine, M.; Houten, J. Van Using paramecium as a model for ciliopathies. *Genes (Basel)* **2021**, *12*, 1493. [CrossRef] [PubMed]
164. Wloga, D.; Camba, A.; Rogowski, K.; Manning, G.; Jerka-Dziadosz, M.; Gaertig, J. Members of the NIMA-related kinase family promote disassembly of cilia by multiple mechanisms. *Mol. Biol. Cell* **2006**, *17*, 2799–2810. [CrossRef] [PubMed]
165. Cezar Alves, H.; da Consolação Diniz Javaroti, D.; Roberto Ferreira, J.; Helena Regali Seleg him, M. Optimized culture and growth curves of two ciliated protozoan strains of *Paramecium caudatum* Ehrenberg, 1833 to use in ecotoxicological assays. *Rev. Bras. Zoociências* **2016**, *17*, 77–90.
166. Ishida, M.; Hori, M. Improved isolation method to establish axenic strains of *Paramecium*. *Japanese J. Protozool.* **2017**, *50*, 1–14. [CrossRef]
167. Gaertig, J.; Wloga, D.; Vasudevan, K.K.; Guha, M.; Dentler, W. Discovery and functional evaluation of ciliary proteins in *Tetrahymena thermophila*. *Methods Enzymol.* **2013**, *525*, 265–284.
168. Jiang, Y.Y.; Lechtreck, K.; Gaertig, J. Total internal reflection fluorescence microscopy of intraflagellar transport in *Tetrahymena thermophila*. *Methods Cell Biol.* **2015**, *127*, 445–456. [CrossRef]
169. Gogendeau, D.; Lemullois, M.; Le Borgne, P.; Castelli, M.; Aubusson-Fleury, A.; Arnaiz, O.; Cohen, J.; Vesque, C.; Schneider-Maunoury, S.; Bouhouche, K.; et al. MKS-NPHP module proteins control ciliary shedding at the transition zone. *PLoS Biol.* **2020**, *18*, e3000640. [CrossRef]
170. Hazime, K.S.; Zhou, Z.; Joachimiak, E.; Bulgakova, N.A.; Wloga, D.; Malicki, J.J. STORM imaging reveals the spatial arrangement of transition zone components and IFT particles at the ciliary base in *Tetrahymena*. *Sci. Rep.* **2021**, *11*, 7899. [CrossRef]
171. Winey, M.; Stemml-Wolf, A.J.; Giddings, T.H.; Pearson, C.G. Cytological Analysis of *Tetrahymena thermophila*. *Methods Cell Biol.* **2012**, *109*, 357–378.
172. Joachimiak, E.; Osinka, A.; Farahat, H.; Świderska, B.; Sitkiewicz, E.; Poprzeczko, M.; Fabczak, H.; Wloga, D. Composition and function of the C1b/C1f region in the ciliary central apparatus. *Sci. Rep.* **2021**, *11*, 11760. [CrossRef]
173. Shang, Y.; Song, X.; Bowen, J.; Corstanje, R.; Gao, Y.; Gaertig, J.; Gorovsky, M.A. A robust inducible-repressible promoter greatly facilitates gene knockouts, conditional expression, and overexpression of homologous and heterologous genes in *Tetrahymena thermophila*. *Proc. Natl. Acad. Sci. USA* **2002**, *99*, 3734–3739. [CrossRef] [PubMed]
174. Dave, D.; Wloga, D.; Gaertig, J. Manipulating ciliary protein-encoding genes in *Tetrahymena thermophila*. *Methods Cell Biol.* **2009**, *93*, 1–20. [CrossRef] [PubMed]
175. Gotesman, M.; Hosein, R.E.; Williams, S.A. Using a Hand-Held Gene Gun for Genetic Transformation of *Tetrahymena thermophila*. *Methods Mol. Biol.* **2022**, *2364*, 349–361. [PubMed]

176. Rajagopalan, V.; Corpuz, E.O.; Hubenschmidt, M.J.; Townsend, C.R.; Asai, D.J.; Wilkes, D.E. Analysis of properties of cilia using *Tetrahymena thermophila*. *Methods Mol. Biol.* **2009**, *586*, 283–299. [CrossRef] [PubMed]
177. Chalker, D.L. Transformation and Strain Engineering of *Tetrahymena*. *Methods Cell Biol.* **2012**, *109*, 327–345.
178. Galvani, A.; Sperling, L. RNA interference by feeding in *Paramecium*. *Trends Genet.* **2002**, *18*, 11–12. [CrossRef]
179. Carradec, Q.; Götz, U.; Arnaiz, O.; Pouch, J.; Simon, M.; Meyer, E.; Marker, S. Primary and secondary siRNA synthesis triggered by RNAs from food bacteria in the ciliate *Paramecium tetraurelia*. *Nucleic Acids Res.* **2015**, *43*, 1818–1833. [CrossRef]
180. Dougherty, G.W.; Loges, N.T.; Klinkenbusch, J.A.; Olbrich, H.; Pennekamp, P.; Menchen, T.; Raidt, J.; Wallmeier, J.; Werner, C.; Westermann, C.; et al. DNAH11 localization in the proximal region of respiratory cilia defines distinct outer dynein arm complexes. *Am. J. Respir. Cell Mol. Biol.* **2016**, *55*, 213–224. [CrossRef]
181. Fliegauf, M.; Olbrich, H.; Horvath, J.; Wildhaber, J.H.; Zariwala, M.A.; Kennedy, M.; Knowles, M.R.; Omran, H. Mislocalization of DNAH5 and DNAH9 in respiratory cells from patients with primary ciliary dyskinesia. *Am. J. Respir. Crit. Care Med.* **2005**, *171*, 1343–1349. [CrossRef]
182. Fassad, M.R.; Shoemark, A.; Legendre, M.; Hirst, R.A.; Koll, F.; le Borgne, P.; Louis, B.; Daudvohra, F.; Patel, M.P.; Thomas, L.; et al. Mutations in Outer Dynein Arm Heavy Chain DNAH9 Cause Motile Cilia Defects and Situs Inversus. *Am. J. Hum. Genet.* **2018**, *103*, 984–994. [CrossRef]
183. Shi, L.; Shen, X.; Chi, Y.; Shen, Y. Primary ciliary dyskinesia relative protein ZMYND10 is involved in regulating ciliary function and intraflagellar transport in *Paramecium tetraurelia*. *Eur. J. Protistol.* **2021**, *77*, 125756. [CrossRef]
184. Thomas, L.; Bouhouche, K.; Whitfield, M.; Thouvenin, G.; Coste, A.; Louis, B.; Szymanski, C.; Bequignon, E.; Papon, J.F.; Castelli, M.; et al. TTC12 Loss-of-Function Mutations Cause Primary Ciliary Dyskinesia and Unveil Distinct Dynein Assembly Mechanisms in Motile Cilia Versus Flagella. *Am. J. Hum. Genet.* **2020**, *106*, 153–169. [CrossRef] [PubMed]
185. Zariwala, M.A.; Gee, H.Y.; Kurkowiak, M.; Al-Mutairi, D.A.; Leigh, M.W.; Hurd, T.W.; Hjeij, R.; Dell, S.D.; Chaki, M.; Dougherty, G.W.; et al. ZMYND10 is mutated in primary ciliary dyskinesia and interacts with LRRC6. *Am. J. Hum. Genet.* **2013**, *93*, 336–345. [CrossRef] [PubMed]
186. Moore, D.J.; Onoufriadiis, A.; Shoemark, A.; Simpson, M.A.; Zur Lage, P.I.; De Castro, S.C.; Bartoloni, L.; Gallone, G.; Petridi, S.; Woppard, W.J.; et al. Mutations in ZMYND10, a gene essential for proper axonemal assembly of inner and outer dynein arms in humans and flies, cause primary ciliary dyskinesia. *Am. J. Hum. Genet.* **2013**, *93*, 346–356. [CrossRef] [PubMed]
187. Kurkowiak, M.; Ziętkiewicz, E.; Greber, A.; Voelkel, K.; Wojda, A.; Pogorzelski, A.; Witt, M. ZMYND10 - Mutation analysis in Slavic patients with primary ciliary dyskinesia. *PLoS ONE* **2016**, *11*, e0148067. [CrossRef]
188. Ziętkiewicz, E.; Bukowy-Bierylo, Z.; Rabiasz, A.; Daca-Roszak, P.; Wojda, A.; Voelkel, K.; Rutkiewicz, E.; Pogorzelski, A.; Rasteiro, M.; Witt, M. CFAP300: Mutations in slavic patients with primary ciliary dyskinesia and a role in ciliary dynein arms trafficking. *Am. J. Respir. Cell Mol. Biol.* **2019**, *61*, 400–449. [CrossRef]
189. Mali, G.R.; Yeyati, P.L.; Mizuno, S.; Dodd, D.O.; Tennant, P.A.; Keighren, M.A.; Lage, P.Z.; Shoemark, A.; Garcia-Munoz, A.; Shimada, A.; et al. ZMYND10 functions in a chaperone relay during axonemal dynein assembly. *Elife* **2018**, *7*, e34389. [CrossRef]
190. Liu, W.; Sha, Y.; Li, Y.; Mei, L.; Lin, S.; Huang, X.; Lu, J.; Ding, L.; Kong, S.; Lu, Z. Loss-of-function mutations in SPEF2 cause multiple morphological abnormalities of the sperm flagella (MMAF). *J. Med. Genet.* **2019**, *56*, 678–684. [CrossRef]
191. Tu, C.; Nie, H.; Meng, L.; Wang, W.; Li, H.; Yuan, S.; Cheng, D.; He, W.; Liu, G.; Du, J.; et al. Novel mutations in SPEF2 causing different defects between flagella and cilia bridge: The phenotypic link between MMAF and PCD. *Hum. Genet.* **2020**, *139*, 257–271. [CrossRef]
192. Liu, C.; Lv, M.; He, X.; Zhu, Y.; Amiri-Yekta, A.; Li, W.; Wu, H.; Kherraf, Z.E.; Liu, W.; Zhang, J.; et al. Homozygous mutations in SPEF2 induce multiple morphological abnormalities of the sperm flagella and male infertility. *J. Med. Genet.* **2020**, *57*, 31–37. [CrossRef]
193. Sha, Y.; Liu, W.; Wei, X.; Zhu, X.; Luo, X.; Liang, L.; Guo, T. Biallelic mutations in Sperm flagellum 2 cause human multiple morphological abnormalities of the sperm flagella (MMAF) phenotype. *Clin. Genet.* **2019**, *96*, 385–393. [CrossRef]
194. Dong, F.N.; Amiri-Yekta, A.; Martinez, G.; Saut, A.; Tek, J.; Stouvenel, L.; Lorès, P.; Karaouzène, T.; Thierry-Mieg, N.; Satre, V.; et al. Absence of CFAP69 Causes Male Infertility due to Multiple Morphological Abnormalities of the Flagella in Human and Mouse. *Am. J. Hum. Genet.* **2018**, *102*, 636–648. [CrossRef] [PubMed]
195. He, X.; Li, W.; Wu, H.; Lv, M.; Liu, W.; Liu, C.; Zhu, F.; Li, C.; Fang, Y.; Yang, C.; et al. Novel homozygous CFAP69 mutations in humans and mice cause severe asthenoteratospermia with multiple morphological abnormalities of the sperm flagella. *J. Med. Genet.* **2019**, *56*, 96–103. [CrossRef] [PubMed]
196. Shen, Q.; Martinez, G.; Liu, H.; Beurois, J.; Wu, H.; Amiri-Yekta, A.; Liang, D.; Kherraf, Z.E.; Bidart, M.; Cazin, C.; et al. Bi-allelic truncating variants in CFAP206 cause male infertility in human and mouse. *Hum. Genet.* **2021**, *140*, 1367–1377. [CrossRef] [PubMed]
197. Jiao, S.Y.; Yang, Y.H.; Chen, S.R. Molecular genetics of infertility: Loss-of-function mutations in humans and corresponding knockout/mutated mice. *Hum. Reprod. Update* **2021**, *27*, 154–189. [CrossRef] [PubMed]
198. Urbanska, P.; Joachimiak, E.; Bazan, R.; Fu, G.; Poprzeczko, M.; Fabczak, H.; Nicastro, D.; Wloga, D. Ciliary proteins Fap43 and Fap44 interact with each other and are essential for proper cilia and flagella beating. *Cell. Mol. Life Sci.* **2018**, *75*, 4479–4493. [CrossRef]

199. Tang, S.; Wang, X.; Li, W.; Yang, X.; Li, Z.; Liu, W.; Li, C.; Zhu, Z.; Wang, L.; Wang, J.; et al. Biallelic Mutations in CFAP43 and CFAP44 Cause Male Infertility with Multiple Morphological Abnormalities of the Sperm Flagella. *Am. J. Hum. Genet.* **2017**, *100*, 854–864. [[CrossRef](#)]
200. Sha, Y.W.; Wang, X.; Xu, X.; Su, Z.Y.; Cui, Y.; Bin Mei, L.; Huang, X.J.; Chen, J.; He, X.M.; Ji, Z.Y.; et al. Novel Mutations in CFAP44 and CFAP43 Cause Multiple Morphological Abnormalities of the Sperm Flagella (MMAF). *Reprod. Sci.* **2019**, *26*, 26–34. [[CrossRef](#)]
201. Khan, I.; Shah, B.; Dil, S.; Ullah, N.; Zhou, J.T.; Zhao, D.R.; Zhang, Y.W.; Jiang, X.H.; Khan, R.; Khan, A.; et al. Novel biallelic loss-of-function mutations in CFAP43 cause multiple morphological abnormalities of the sperm flagellum in Pakistani families. *Asian J. Androl.* **2021**, *23*, 627–632. [[CrossRef](#)]
202. Wu, H.; Li, W.; He, X.; Liu, C.; Fang, Y.; Zhu, F.; Jiang, H.; Liu, W.; Song, B.; Wang, X.; et al. Novel CFAP43 and CFAP44 mutations cause male infertility with multiple morphological abnormalities of the sperm flagella (MMAF). *Reprod. Biomed. Online* **2019**, *38*, 769–778. [[CrossRef](#)]
203. Liu, S.; Zhang, J.; Kherraf, Z.E.; Sun, S.; Zhang, X.; Cazin, C.; Coutton, C.; Zouari, R.; Zhao, S.; Hu, F.; et al. CFAP61 is required for sperm flagellum formation and male fertility in human and mouse. *Development* **2021**, *148*, dev199805. [[CrossRef](#)]
204. Urbanska, P.; Song, K.; Joachimiak, E.; Krzemien-Ojak, L.; Koprowski, P.; Hennessey, T.; Jerka-Dziadosz, M.; Fabczak, H.; Gaertig, J.; Nicastro, D.; et al. The CSC proteins FAP61 and FAP251 build the basal substructures of radial spoke 3 in cilia. *Mol. Biol. Cell* **2015**, *26*, 1463–1475. [[CrossRef](#)] [[PubMed](#)]
205. Li, W.; He, X.; Yang, S.; Liu, C.; Wu, H.; Liu, W.; Lv, M.; Tang, D.; Tan, J.; Tang, S.; et al. Biallelic mutations of CFAP251 cause sperm flagellar defects and human male infertility. *J. Hum. Genet.* **2019**, *64*, 49–54. [[CrossRef](#)] [[PubMed](#)]
206. Lobo, D.; Beane, W.S.; Levin, M. Modeling planarian regeneration: A primer for reverse-engineering the worm. *PLoS Comput. Biol.* **2012**, *8*, e1002481. [[CrossRef](#)]
207. Azimzadeh, J.; Basquin, C. Basal bodies across eukaryotes series: Basal bodies in the freshwater planarian Schmidtea mediterranea. *Cilia* **2016**, *5*, 15. [[CrossRef](#)] [[PubMed](#)]
208. Li, Y.; Guo, F.; Jing, Q.; Zhu, X.; Yan, X. Characterisation of centriole biogenesis during multiciliation in planarians. *Biol. Cell* **2020**, *112*, 398–408. [[CrossRef](#)]
209. Lesko, S.L.; Rouhana, L. Dynein assembly factor with WD repeat domains 1 (DAW1) is required for the function of motile cilia in the planarian Schmidtea mediterranea. *Dev. Growth Differ.* **2020**, *62*, 423–437. [[CrossRef](#)]
210. Kyuji, A.; Patel-King, R.S.; Hisabori, T.; King, S.M.; Wakabayashi, K.I. Cilia Loss and Dynein Assembly Defects in Planaria Lacking an Outer Dynein Arm-Docking Complex Subunit. *Zoolog. Sci.* **2020**, *37*, 7–13. [[CrossRef](#)]
211. Basquin, C.; Orfila, A.M.; Azimzadeh, J. The planarian Schmidtea mediterranea as a model for studying motile cilia and multiciliated cells. *Methods Cell Biol.* **2015**, *127*, 243–262. [[CrossRef](#)]
212. Rink, J.C.; Vu, H.T.K.; Alvarado, A.S. The maintenance and regeneration of the planarian excretory system are regulated by EGFR signaling. *Development* **2011**, *138*, 3769–3780. [[CrossRef](#)]
213. McKenna, J.A. Fine structure of the protonephridial system in planaria - I. Flame cells. *Zeitschrift für Zellforsch. Mikroskopische Anat.* **1968**, *92*, 509–523. [[CrossRef](#)]
214. MacRae, E.K. The fine structure of sensory receptor processes in the auricular epithelium of the planarian, *Dugesia tigrina*. *Zeitschrift für Zellforsch. Mikroskopische Anat.* **1967**, *82*, 479–494. [[CrossRef](#)] [[PubMed](#)]
215. Brooks, E.R.; Wallingford, J.B. Multiciliated Cells. *Curr. Biol.* **2014**, *24*, R973–R982. [[CrossRef](#)] [[PubMed](#)]
216. Merryman, M.S.; Alvarado, A.S.; Jenkins, J.C. Culturing planarians in the laboratory. *Methods Mol. Biol.* **2018**, *1774*, 241–258. [[PubMed](#)]
217. Sousa, N.; Adell, T. Maintenance of Schmidtea mediterranea in the Laboratory. *BIO-PROTOCOL* **2018**, *8*, e3040. [[CrossRef](#)]
218. Rompolas, P.; Azimzadeh, J.; Marshall, W.F.; King, S.M. Analysis of ciliary assembly and function in planaria. *Methods Enzymol.* **2013**, *525*, 245–264.
219. King, S.M.; Patel-King, R.S. Planaria as a model system for the analysis of ciliary assembly and motility. *Methods Mol. Biol.* **2016**, *1454*, 245–254.
220. Vij, S.; Rink, J.C.; Ho, H.K.; Babu, D.; Eitel, M.; Narasimhan, V.; Tiku, V.; Westbrook, J.; Schierwater, B.; Roy, S. Evolutionarily Ancient Association of the FoxJ1 Transcription Factor with the Motile Ciliogenic Program. *PLoS Genet.* **2012**, *8*, e1003019. [[CrossRef](#)]
221. Höben, I.M.; Hjeij, R.; Olbrich, H.; Dougherty, G.W.; Nöthe-Mench, T.; Aprea, I.; Frank, D.; Pennekamp, P.; Dworniczak, B.; Wallmeier, J.; et al. Mutations in C11orf70 Cause Primary Ciliary Dyskinesia with Randomization of Left/Right Body Asymmetry Due to Defects of Outer and Inner Dynein Arms. *Am. J. Hum. Genet.* **2018**, *102*, 973–984. [[CrossRef](#)]
222. Ahmed, N.T.; Gao, C.; Lucker, B.F.; Cole, D.G.; Mitchell, D.R. ODA16 aids axonemal outer row dynein assembly through an interaction with the intraflagellar transport machinery. *J. Cell Biol.* **2008**, *183*, 313–322. [[CrossRef](#)]
223. Taschner, M.; Mourão, A.; Awasthi, M.; Basquin, J.; Lorentzen, E. Structural basis of outer dynein arm intraflagellar transport by the transport adaptor protein ODA16 and the intraflagellar transport protein IFT46. *J. Biol. Chem.* **2017**, *292*, 7462–7473. [[CrossRef](#)]
224. Hou, Y.; Witman, G.B. The N-terminus of IFT46 mediates intraflagellar transport of outer arm dynein and its cargo-adaptor ODA16. *Mol. Biol. Cell* **2017**, *28*, 2420–2433. [[CrossRef](#)] [[PubMed](#)]
225. Ahmed, N.T.; Mitchell, D.R. ODA16p, a chlamydomonas flagellar protein needed for dynein assembly. *Mol. Biol. Cell* **2005**, *16*, 5004–5012. [[CrossRef](#)] [[PubMed](#)]

226. Gao, C.; Wang, G.; Amack, J.D.; Mitchell, D.R. Oda16/Wdr69 is essential for axonemal dynein assembly and ciliary motility during zebrafish embryogenesis. *Dev. Dyn.* **2010**, *239*, 2190–2197. [CrossRef] [PubMed]
227. Solomon, G.M.; Francis, R.; Chu, K.K.; Birket, S.E.; Gabriel, G.; Trombley, J.E.; Lemke, K.L.; Klena, N.; Turner, B.; Tearney, G.J.; et al. Assessment of ciliary phenotype in primary ciliary dyskinesia by micro-optical coherence tomography. *JCI insight* **2017**, *2*, e91702. [CrossRef] [PubMed]
228. Kimmel, C.B.; Ballard, W.W.; Kimmel, S.R.; Ullmann, B.; Schilling, T.F. Stages of embryonic development of the zebrafish. *Dev. Dyn.* **1995**, *203*, 253–310. [CrossRef]
229. Kalueff, A.V.; Stewart, A.M.; Gerlai, R. Zebrafish as an emerging model for studying complex brain disorders. *Trends Pharmacol. Sci.* **2014**, *35*, 63–75. [CrossRef]
230. Olmstead, A.W.; Korte, J.J.; Woodis, K.K.; Bennett, B.A.; Ostazeski, S.; Degitz, S.J. Reproductive maturation of the tropical clawed frog: *Xenopus tropicalis*. *Gen. Comp. Endocrinol.* **2009**, *160*, 117–123. [CrossRef]
231. Wlizla, M.; McNamara, S.; Horb, M.E. Generation and care of *Xenopus laevis* and *Xenopus tropicalis* embryos. *Methods Mol. Biol.* **2018**, *1865*, 19–32.
232. Blitz, I.L.; Cho, K.W.Y. Control of zygotic genome activation in *Xenopus*. *Curr. Top. Dev. Biol.* **2021**, *145*, 167–204. [CrossRef]
233. Blum, M.; Ott, T. Xenopus: An undervalued model organism to study and model human genetic disease. *Cells Tissues Organs* **2019**, *205*, 303–312. [CrossRef]
234. Session, A.M.; Uno, Y.; Kwon, T.; Chapman, J.A.; Toyoda, A.; Takahashi, S.; Fukui, A.; Hikosaka, A.; Suzuki, A.; Kondo, M.; et al. Genome evolution in the allotetraploid frog *Xenopus laevis*. *Nature* **2016**, *538*, 336–343. [CrossRef] [PubMed]
235. Kostiuk, V.; Khokha, M.K. Xenopus as a platform for discovery of genes relevant to human disease. *Curr. Top. Dev. Biol.* **2021**, *145*, 277–312. [CrossRef] [PubMed]
236. Kramer-Zucker, A.G.; Olale, F.; Haycraft, C.J.; Yoder, B.K.; Schier, A.F.; Drummond, I.A. Cilia-driven fluid flow in the zebrafish pronephros, brain and Kupffer's vesicle is required for normal organogenesis. *Development* **2005**, *132*, 1907–1921. [CrossRef] [PubMed]
237. Tavares, B.; Jacinto, R.; Sampaio, P.; Pestana, S.; Pinto, A.; Vaz, A.; Roxo-Rosa, M.; Gardner, R.; Lopes, T.; Schilling, B.; et al. Notch/Her12 signalling modulates, motile/immotile cilia ratio downstream of Foxj1a in zebrafish left-right organizer. *Elife* **2017**, *6*, e25165. [CrossRef] [PubMed]
238. Fox, C.; Manning, M.L.; Amack, J.D. Quantitative description of fluid flows produced by left-right cilia in zebrafish. *Methods Cell Biol.* **2015**, *127*, 175–187. [CrossRef] [PubMed]
239. Ruzicka, L.; Howe, D.G.; Ramachandran, S.; Toro, S.; Van Slyke, C.E.; Bradford, Y.M.; Eagle, A.; Fashena, D.; Frazer, K.; Kalita, P.; et al. The Zebrafish Information Network: New support for non-coding genes, richer Gene Ontology annotations and the Alliance of Genome Resources. *Nucleic Acids Res.* **2019**, *47*, D867–D873. [CrossRef]
240. Bowes, J.B.; Snyder, K.A.; Segerdell, E.; Gibb, R.; Jarabek, C.; Noumen, E.; Pollet, N.; Vize, P.D. Xenbase: A xenopus biology and genomics resource. *Nucleic Acids Res.* **2008**, *36*, D761–D767. [CrossRef]
241. Olstad, E.W.; Ringers, C.; Hansen, J.N.; Wens, A.; Brandt, C.; Wachten, D.; Yaksi, E.; Jurisch-Yaksi, N. Ciliary Beating Compartmentalizes Cerebrospinal Fluid Flow in the Brain and Regulates Ventricular Development. *Curr. Biol.* **2019**, *29*, 229–241. [CrossRef]
242. Pinto, A.L.; Rasteiro, M.; Bota, C.; Pestana, S.; Sampaio, P.; Hogg, C.; Burgoyne, T.; Lopes, S.S. Zebrafish motile cilia as a model for primary ciliary dyskinesia. *Int. J. Mol. Sci.* **2021**, *22*, 8361. [CrossRef]
243. Liu, Y.; Pathak, N.; Kramer-Zucker, A.; Drummond, I.A. Notch signaling controls the differentiation of transporting epithelia and multiciliated cells in the zebrafish pronephros. *Development* **2007**, *134*, 1111–1122. [CrossRef]
244. Cao, Y.; Park, A.; Sun, Z. Intraflagellar transport proteins are essential for cilia formation and for planar cell polarity. *J. Am. Soc. Nephrol.* **2010**, *21*, 1326–1333. [CrossRef]
245. Malicki, J.; Avanesov, A.; Li, J.; Yuan, S.; Sun, Z. Analysis of Cilia Structure and Function in Zebrafish. *Methods Cell Biol.* **2011**, *101*, 39–74. [CrossRef] [PubMed]
246. Song, Z.; Zhang, X.; Jia, S.; Yelick, P.C.; Zhao, C. Zebrafish as a Model for Human Ciliopathies. *J. Genet. Genomics* **2016**, *43*, 107–120. [CrossRef] [PubMed]
247. Boskovski, M.T.; Yuan, S.; Pedersen, N.B.; Goth, C.K.; Makova, S.; Clausen, H.; Brueckner, M.; Khokha, M.K. The heterotaxy gene GALNT11 glycosylates Notch to orchestrate cilia type and laterality. *Nature* **2013**, *504*, 456–459. [CrossRef]
248. Blum, M.; Beyer, T.; Weber, T.; Vick, P.; Andre, P.; Bitzer, E.; Schweickert, A. Xenopus, an ideal model system to study vertebrate left-right asymmetry. *Dev. Dyn.* **2009**, *238*, 1215–1225. [CrossRef]
249. Schweickert, A.; Weber, T.; Beyer, T.; Vick, P.; Bogusch, S.; Feistel, K.; Blum, M. Cilia-Driven Leftward Flow Determines Laterality in Xenopus. *Curr. Biol.* **2007**, *17*, 60–66. [CrossRef]
250. Chung, M.I.; Peyrot, S.M.; LeBoeuf, S.; Park, T.J.; McGary, K.L.; Marcotte, E.M.; Wallingford, J.B. RFX2 is broadly required for ciliogenesis during vertebrate development. *Dev. Biol.* **2012**, *363*, 155–165. [CrossRef]
251. Rao, V.G.; Kulkarni, S.S. Xenopus to the rescue: A model to validate and characterize candidate ciliopathy genes. *Genesis* **2021**, *59*, e23414. [CrossRef]
252. Werner, M.E.; Mitchell, B.J. Understanding ciliated epithelia: The power of Xenopus. *Genesis* **2012**, *50*, 176–185. [CrossRef] [PubMed]
253. Zhang, S.; Mitchell, B.J. Basal bodies in Xenopus. *Cilia* **2016**, *5*, 2. [CrossRef]

254. Wallmeier, J.; Shiratori, H.; Dougherty, G.W.; Edelbusch, C.; Hjeij, R.; Loges, N.T.; Menchen, T.; Olbrich, H.; Pennekamp, P.; Raidt, J.; et al. TTC25 Deficiency Results in Defects of the Outer Dynein Arm Docking Machinery and Primary Ciliary Dyskinesia with Left-Right Body Asymmetry Randomization. *Am. J. Hum. Genet.* **2016**, *99*, 460–469. [CrossRef] [PubMed]
255. Schweickert, A.; Feistel, K. The Xenopus Embryo: An Ideal Model System to Study Human Ciliopathies. *Curr. Pathobiol. Rep.* **2015**, *32*, 2015, 3, 115–127. [CrossRef]
256. Werner, M.E.; Mitchell, B.J. Using xenopus skin to study cilia development and function. *Methods Enzymol.* **2013**, *525*, 191–217.
257. Walentek, P.; Quigley, I.K. What we can learn from a tadpole about ciliopathies and airway diseases: Using systems biology in Xenopus to study cilia and mucociliary epithelia. *Genesis* **2017**, *55*, e23001. [CrossRef] [PubMed]
258. Hagenlocher, C.; Walentek, P.; Müller, C.; Thumberger, T.; Feistel, K. Ciliogenesis and cerebrospinal fluid flow in the developing Xenopus brain are regulated by foxj1. *Cilia* **2013**, *2*, 12. [CrossRef] [PubMed]
259. Leventea, E.; Hazime, K.; Zhao, C.; Malicki, J. Analysis of cilia structure and function in zebrafish. *Methods Cell Biol.* **2016**, *133*, 179–227. [CrossRef]
260. Brooks, E.R.; Wallingford, J.B. In vivo investigation of cilia structure and function using Xenopus. *Methods Cell Biol.* **2015**, *127*, 131–159. [CrossRef]
261. Heasman, J. Morpholino oligos: Making sense of antisense? *Dev. Biol.* **2002**, *243*, 209–214. [CrossRef]
262. Auer, T.O.; Bene, F. Del CRISPR/Cas9 and TALEN-mediated knock-in approaches in zebrafish. *Methods* **2014**, *69*, 142–150. [CrossRef]
263. Tandon, P.; Conlon, F.; Furlow, J.D.; Horb, M.E. Expanding the genetic toolkit in Xenopus: Approaches and opportunities for human disease modeling. *Dev. Biol.* **2017**, *426*, 325–335. [CrossRef]
264. Salanga, C.M.; Salanga, M.C. Genotype to phenotype: Crispr gene editing reveals genetic compensation as a mechanism for phenotypic disjunction of morphants and mutants. *Int. J. Mol. Sci.* **2021**, *22*, 3472. [CrossRef] [PubMed]
265. Yu, X.; Ng, C.P.; Habacher, H.; Roy, S. Foxj1 transcription factors are master regulators of the motile ciliogenic program. *Nat. Genet.* **2008**, *40*, 1445–1453. [CrossRef] [PubMed]
266. Stubbs, J.L.; Oishi, I.; Belmonte, J.C.I.; Kintner, C. The forkhead protein Foxj1 specifies node-like cilia in Xenopus and zebrafish embryos. *Nat. Genet.* **2008**, *40*, 1454–1460. [CrossRef] [PubMed]
267. Zhou, F.; Rayamajhi, D.; Ravi, V.; Narasimhan, V.; Chong, Y.L.; Lu, H.; Venkatesh, B.; Roy, S. Conservation as well as divergence in Mcidas function underlies the differentiation of multiciliated cells in vertebrates. *Dev. Biol.* **2020**, *465*, 168–177. [CrossRef] [PubMed]
268. Hjeij, R.; Onoufriadiis, A.; Watson, C.M.; Slagle, C.E.; Klena, N.T.; Dougherty, G.W.; Kurkowiak, M.; Loges, N.T.; Diggle, C.P.; Morante, N.F.C.; et al. CCDC151 mutations cause primary ciliary dyskinesia by disruption of the outer dynein arm docking complex formation. *Am. J. Hum. Genet.* **2014**, *95*, 257–274. [CrossRef]
269. Hjeij, R.; Lindstrand, A.; Francis, R.; Zariwala, M.A.; Liu, X.; Li, Y.; Damerla, R.; Dougherty, G.W.; Abouhamed, M.; Olbrich, H.; et al. ARMC4 mutations cause primary ciliary dyskinesia with randomization of left/right body asymmetry. *Am. J. Hum. Genet.* **2013**, *93*, 357–367. [CrossRef]
270. Xu, Y.; Cao, J.; Huang, S.; Feng, D.; Zhang, W.; Zhu, X.; Yan, X. Characterization of tetratricopeptide repeat-containing proteins critical for cilia formation and function. *PLoS ONE* **2015**, *10*, e0124378. [CrossRef]
271. Becker-Heck, A.; Zohn, I.E.; Okabe, N.; Pollock, A.; Lenhart, K.B.; Sullivan-Brown, J.; McSheene, J.; Loges, N.T.; Olbrich, H.; Haefner, K.; et al. The coiled-coil domain containing protein CCDC40 is essential for motile cilia function and left-right axis formation. *Nat. Genet.* **2011**, *43*, 79–84. [CrossRef]
272. Colantonio, J.R.; Vermot, J.; Wu, D.; Langenbacher, A.D.; Fraser, S.; Chen, J.N.; Hill, K.L. The dynein regulatory complex is required for ciliary motility and otolith biogenesis in the inner ear. *Nature* **2009**, *457*, 205–209. [CrossRef]
273. Evron, T.; Philipp, M.; Lu, J.; Meloni, A.R.; Burkhalter, M.; Chen, W.; Caron, M.G. Growth arrest specific 8 (Gas8) and G protein-coupled receptor kinase 2 (GRK2) cooperate in the control of smoothened signaling. *J. Biol. Chem.* **2011**, *286*, 27676–27686. [CrossRef]
274. Sedykh, I.; Teslala, J.J.; Tatarsky, R.L.; Keller, A.N.; Toops, K.A.; Lakkaraju, A.; Nyholm, M.K.; Wolman, M.A.; Grinblat, Y. Novel roles for the radial spoke head protein 9 in neural and neurosensory cilia. *Sci. Rep.* **2016**, *6*, 34437. [CrossRef] [PubMed]
275. Cho, E.H.; Huh, H.J.; Jeong, I.; Lee, N.Y.; Koh, W.J.; Park, H.C.; Ki, C.S. A nonsense variant in NME5 causes human primary ciliary dyskinesia with radial spoke defects. *Clin. Genet.* **2020**, *98*, 64–68. [CrossRef] [PubMed]
276. Wilson, C.W.; Nguyen, C.T.; Chen, M.H.; Yang, J.H.; Gacayan, R.; Huang, J.; Chen, J.N.; Chuang, P.T. Fused has evolved divergent roles in vertebrate Hedgehog signalling and motile ciliogenesis. *Nature* **2009**, *459*, 98–102. [CrossRef] [PubMed]
277. Falkenberg, L.G.; Beckman, S.A.; Ravisankar, P.; Dohn, T.E.; Waxman, J.S. Ccdc103 promotes myeloid cell proliferation and migration independent of motile cilia. *DMM Dis. Model. Mech.* **2021**, *14*, dmm048439. [CrossRef]
278. Pazour, G.J.; Witman, G.B. The vertebrate primary cilium is a sensory organelle. *Curr. Opin. Cell Biol.* **2003**, *15*, 105–110. [CrossRef]
279. Afzelius, B.A.; Ewetz, L.; Palmblad, J.; Udén, A.-M.; Venizelos, N. Structure and Function of Neutrophil Leukocytes from Patients with the Immotile-Cilia Syndrome. *Acta Med. Scand.* **1980**, *208*, 145–154. [CrossRef]
280. Cockx, M.; Gouwy, M.; Ruytin, P.; Lodewijckx, I.; Van Hout, A.; Knoops, S.; Pörtner, N.; Ronsse, I.; Vanbrabant, L.; Godding, V.; et al. Monocytes from patients with Primary Ciliary Dyskinesia show enhanced inflammatory properties and produce higher levels of pro-inflammatory cytokines. *Sci. Rep.* **2017**, *7*, 14657. [CrossRef]

281. Cockx, M.; Blanter, M.; Gouwy, M.; Ruytinx, P.; Salama, S.A.; Knoops, S.; Pörtner, N.; Vanbrabant, L.; Lorent, N.; Boon, M.; et al. The antimicrobial activity of peripheral blood neutrophils is altered in patients with primary ciliary dyskinesia. *Int. J. Mol. Sci.* **2021**, *22*, 6172. [CrossRef]
282. Stubbs, J.L.; Vladar, E.K.; Axelrod, J.D.; Kintner, C. Multicilin promotes centriole assembly and ciliogenesis during multiciliate cell differentiation. *Nat. Cell Biol.* **2012**, *14*, 140–147. [CrossRef]
283. Wallmeier, J.; Al-Mutairi, D.A.; Chen, C.T.; Loges, N.T.; Pennekamp, P.; Menchen, T.; Ma, L.; Shamseldin, H.E.; Olbrich, H.; Dougherty, G.W.; et al. Mutations in CCNO result in congenital mucociliary clearance disorder with reduced generation of multiple motile cilia. *Nat. Genet.* **2014**, *46*, 646–651. [CrossRef]
284. Amirav, I.; Wallmeier, J.; Loges, N.T.; Menchen, T.; Pennekamp, P.; Mussaffi, H.; Abitbul, R.; Avital, A.; Bentur, L.; Dougherty, G.W.; et al. Systematic Analysis of CCNO Variants in a Defined Population: Implications for Clinical Phenotype and Differential Diagnosis. *Hum. Mutat.* **2016**, *37*, 396–405. [CrossRef] [PubMed]
285. Jaffe, K.M.; Grimes, D.T.; Schottenfeld-Roames, J.; Werner, M.E.; Ku, T.S.J.; Kim, S.K.; Pelliccia, J.L.; Morante, N.F.C.; Mitchell, B.J.; Burdine, R.D. C21orf59/kurly Controls Both Cilia Motility and Polarization. *Cell Rep.* **2016**, *14*, 1841–1849. [CrossRef]
286. Rachev, E.; Schuster-Gossler, K.; Fuhl, F.; Ott, T.; Tveriakhina, L.; Beckers, A.; Hegermann, J.; Boldt, K.; Mai, M.; Kremmer, E.; et al. CFAP43 modulates ciliary beating in mouse and Xenopus. *Dev. Biol.* **2020**, *459*, 109–125. [CrossRef] [PubMed]
287. Lee, L.; Ostrowski, L.E. Motile cilia genetics and cell biology: Big results from little mice. *Cell. Mol. Life Sci.* **2021**, *78*, 769–797. [CrossRef] [PubMed]
288. Sosa, M.A.G.; De Gasperi, R.; Elder, G.A. Modeling human neurodegenerative diseases in transgenic systems. *Hum. Genet.* **2012**, *131*, 535–563. [CrossRef]
289. Vincensini, L.; Blisnick, T.; Bastin, P. 1001 Model Organisms To Study Cilia and Flagella. *Biol. Cell* **2011**, *103*, 109–130. [CrossRef]
290. Peters, L.L.; Robledo, R.F.; Bult, C.J.; Churchill, G.A.; Paigen, B.J.; Svenson, K.L. The mouse as a model for human biology: A resource guide for complex trait analysis. *Nat. Rev. Genet.* **2007**, *8*, 58–69. [CrossRef]
291. Rosenthal, N.; Brown, S. The mouse ascending: Perspectives for human-disease models. *Nat. Cell Biol.* **2007**, *9*, 993–999. [CrossRef]
292. Vladar, E.K.; Brody, S.L. Analysis of Ciliogenesis in Primary Culture Mouse Tracheal Epithelial Cells. *Methods Enzymol.* **2013**, *525*, 285–309.
293. Eenjes, E.; Mertens, T.C.J.; Buscop-Van Kempen, M.J.; Van Wijck, Y.; Taube, C.; Rottier, R.J.; Hiemstra, P.S. A novel method for expansion and differentiation of mouse tracheal epithelial cells in culture. *Sci. Rep.* **2018**, *8*, 7349. [CrossRef]
294. Gabrion, J.B.; Herbuté, S.; Bouillé, C.; Maurel, D.; Kuchler-Bopp, S.; Laabich, A.; Delaunoy, J.P. Ependymal and choroidal cells in culture: Characterization and functional differentiation. *Microsc. Res. Tech.* **1998**, *41*, 124–157. [CrossRef]
295. Delgehyr, N.; Meunier, A.; Faucourt, M.; Grau, M.B.; Strehl, L.; Janke, C.; Spassky, N. Ependymal cell differentiation, from monociliated to multiciliated cells. *Methods Cell Biol.* **2015**, *127*, 19–35. [CrossRef] [PubMed]
296. Grondona, J.M.; Granados-Durán, P.; Fernández-Llebrez, P.; López-Ávalos, M.D. A simple method to obtain pure cultures of multiciliated ependymal cells from adult rodents. *Histochem. Cell Biol.* **2013**, *139*, 205–220. [CrossRef] [PubMed]
297. Tan, S.Y.; Rosenthal, J.; Zhao, X.-Q.; Francis, R.J.; Chatterjee, B.; Sabol, S.L.; Linask, K.L.; Bracero, L.; Connelly, P.S.; Daniels, M.P.; et al. Heterotaxy and complex structural heart defects in a mutant mouse model of primary ciliary dyskinesia. *J. Clin. Invest.* **2007**, *117*, 3742–3752. [CrossRef]
298. Ermakov, A.; Stevens, J.L.; Whitehill, E.; Robson, J.E.; Pieles, G.; Brooker, D.; Goggolidou, P.; Powles-Glover, N.; Hacker, T.; Young, S.R.; et al. Mouse mutagenesis identifies novel roles for left-right patterning genes in pulmonary, craniofacial, ocular, and limb development. *Dev. Dyn.* **2009**, *238*, 581–594. [CrossRef]
299. Burnicka-Turek, O.; Steimle, J.D.; Huang, W.; Felker, L.; Kamp, A.; Kweon, J.; Peterson, M.; Reeves, R.H.; Maslen, C.L.; Gruber, P.J.; et al. Cilia gene mutations cause atrioventricular septal defects by multiple mechanisms. *Hum. Mol. Genet.* **2016**, *25*, 3011–3028. [CrossRef] [PubMed]
300. Abdelhamed, Z.; Vuong, S.M.; Hill, L.; Shula, C.; Timms, A.; Beier, D.; Campbell, K.; Mangano, F.T.; Stottmann, R.W.; Goto, J. A mutation in Ccdc39 causes neonatal hydrocephalus with abnormal motile cilia development in mice. *Development* **2018**, *145*, dev154500. [CrossRef]
301. Ha, S.; Lindsay, A.M.; Timms, A.E.; Beier, D.R. Mutations in Dnaaf1 and Lrrc48 cause hydrocephalus, laterality defects, and sinusitis in mice. *G3 Genes, Genomes, Genet.* **2016**, *6*, 2479–2487. [CrossRef]
302. Sironen, A.; Kotaja, N.; Mulhern, H.; Wyatt, T.A.; Sisson, J.H.; Pavlik, J.A.; Miiluniemi, M.; Fleming, M.D.; Lee, L. Loss of SPEF2 function in mice results in spermatogenesis defects and primary ciliary dyskinesia. *Biol. Reprod.* **2011**, *85*, 690–701. [CrossRef]
303. Cheong, A.; Degani, R.; Tremblay, K.D.; Mager, J. A null allele of Dnaaf2 displays embryonic lethality and mimics human ciliary dyskinesia. *Hum. Mol. Genet.* **2019**, *28*, 2775–2784. [CrossRef]
304. Matsuo, M.; Shimada, A.; Koshida, S.; Saga, Y.; Takeda, H. The establishment of rotational polarity in the airway and ependymal cilia: Analysis with a novel cilium motility mutant mouse. *Am. J. Physiol.-Lung Cell. Mol. Physiol.* **2013**, *304*, L736–L745. [CrossRef]
305. Yin, W.; Livraghi-Butrico, A.; Sears, P.R.; Rogers, T.D.; Burns, K.A.; Grubb, B.R.; Ostrowski, L.E. Mice with a deletion of Rspn1 exhibit a low level of mucociliary clearance and develop a primary ciliary dyskinesia phenotype. *Am. J. Respir. Cell Mol. Biol.* **2019**, *61*, 312–321. [CrossRef] [PubMed]
306. Tarkar, A.; Loges, N.T.; Slagle, C.E.; Francis, R.; Dougherty, G.W.; Tamayo, J.V.; Shook, B.; Cantino, M.; Schwartz, D.; Jahnke, C.; et al. DYX1C1 is required for axonemal dynein assembly and ciliary motility. *Nat. Genet.* **2013**, *45*, 995–1003. [CrossRef] [PubMed]

307. Lehti, M.S.; Henriksson, H.; Rummukainen, P.; Wang, F.; Uusitalo-Kylmälä, L.; Kiviranta, R.; Heino, T.J.; Kotaja, N.; Sironen, A. Cilia-related protein SPEF2 regulates osteoblast differentiation. *Sci. Rep.* **2018**, *8*, 859. [[CrossRef](#)] [[PubMed](#)]
308. Lehti, M.S.; Zhang, F.P.; Kotaja, N.; Sironen, A. SPEF2 functions in microtubule-mediated transport in elongating spermatids to ensure proper male germ cell differentiation. *Development* **2017**, *144*, 2683–2693. [[CrossRef](#)]
309. Oji, A.; Noda, T.; Fujihara, Y.; Miyata, H.; Kim, Y.J.; Muto, M.; Nozawa, K.; Matsumura, T.; Isotani, A.; Ikawa, M. CRISPR/Cas9 mediated genome editing in ES cells and its application for chimeric analysis in mice. *Sci. Rep.* **2016**, *6*, 31666. [[CrossRef](#)]
310. Lu, H.; Anujan, P.; Zhou, F.; Zhang, Y.; Chong, Y.L.; Bingle, C.D.; Roy, S. Mcidas mutant mice reveal a two-step process for the specification and differentiation of multiciliated cells in mammals. *Development* **2019**, *146*, dev172643. [[CrossRef](#)]
311. Muthusamy, N.; Vijayakumar, A.; Cheng, G.; Ghashghaei, H.T. A Knock-in Foxj1CreERT2:: GFP mouse for recombination in epithelial cells with motile cilia. *Genesis* **2014**, *52*, 350–358. [[CrossRef](#)]
312. Schmitz, F.; Burtscher, I.; Stauber, M.; Gossler, A.; Lickert, H. A novel Cre-inducible knock-in ARL13B-tRFP fusion cilium reporter. *Genesis* **2017**, *55*, e23073. [[CrossRef](#)]
313. Hua, X.; Zeman, K.L.; Zhou, B.; Hua, Q.; Senior, B.A.; Tilley, S.L.; Bennett, W.D. Noninvasive real-time measurement of nasal mucociliary clearance in mice by pinhole gamma scintigraphy. *J. Appl. Physiol.* **2010**, *108*, 189–196. [[CrossRef](#)]
314. Grubb, B.R.; Livraghi-Butrico, A.; Rogers, T.D.; Yin, W.; Button, B.; Ostrowski, L.E. Reduced mucociliary clearance in old mice is associated with a decrease in muc5b mucin. *Am. J. Physiol.-Lung Cell. Mol. Physiol.* **2016**, *310*, L860–L867. [[CrossRef](#)]
315. Veres, T.Z.; Kopcsányi, T.; Tirri, M.; Braun, A.; Miyasaka, M.; Germain, R.N.; Jalkanen, S.; Salmi, M. Intubation-free in vivo imaging of the tracheal mucosa using two-photon microscopy. *Sci. Rep.* **2017**, *7*, 694. [[CrossRef](#)] [[PubMed](#)]
316. Donnelley, M.; Morgan, K.S.; Siu, K.K.W.; Fouras, A.; Farrow, N.R.; Carnibella, R.P.; Parsons, D.W. Tracking extended mucociliary transport activity of individual deposited particles: Longitudinal synchrotron X-ray imaging in live mice. *J. Synchrotron Radiat.* **2014**, *21*, 768–773. [[CrossRef](#)] [[PubMed](#)]
317. Liu, T.; Jin, X.; Prasad, R.M.; Sari, Y.; Nauli, S.M. Three types of ependymal cells with intracellular calcium oscillation are characterized by distinct cilia beating properties. *J. Neurosci. Res.* **2014**, *92*, 1199–1204. [[CrossRef](#)]
318. Ansari, R.; Buj, C.; Pieper, M.; König, P.; Schweikard, A.; Hüttmann, G. Micro-anatomical and functional assessment of ciliated epithelium in mouse trachea using optical coherence phase microscopy. *Opt. Express* **2015**, *23*, 23217. [[CrossRef](#)]
319. Lee, L. Riding the wave of ependymal cilia: Genetic susceptibility to hydrocephalus in primary ciliary dyskinesia. *J. Neurosci. Res.* **2013**, *91*, 1117–1132. [[CrossRef](#)] [[PubMed](#)]
320. Finn, R.; Evans, C.C.; Lee, L. Strain-dependent brain defects in mouse models of primary ciliary dyskinesia with mutations in Pcdp1 and Spef2. *Neuroscience* **2014**, *277*, 552–567. [[CrossRef](#)]
321. McKenzie, C.W.; Preston, C.C.; Finn, R.; Eyster, K.M.; Faustino, R.S.; Lee, L. Strain-specific differences in brain gene expression in a hydrocephalic mouse model with motile cilia dysfunction. *Sci. Rep.* **2018**, *8*, 13370. [[CrossRef](#)]
322. Dixon, M.; Shoemark, A. Secondary defects detected by transmission electron microscopy in primary ciliary dyskinesia diagnostics. *Ultrastruct. Pathol.* **2017**, *41*, 390–398. [[CrossRef](#)]
323. Hirst, R.A.; Jackson, C.L.; Coles, J.L.; Williams, G.; Rutman, A.; Goggin, P.M.; Adam, E.C.; Page, A.; Evans, H.J.; Lackie, P.M.; et al. Culture of Primary Ciliary Dyskinesia Epithelial Cells at Air-Liquid Interface Can Alter Ciliary Phenotype but Remains a Robust and Informative Diagnostic Aid. *PLoS ONE* **2014**, *9*, e89675. [[CrossRef](#)]
324. Coles, J.L.; Thompson, J.; Horton, K.L.; Hirst, R.A.; Griffin, P.; Williams, G.M.; Goggin, P.; Doherty, R.; Lackie, P.M.; Harris, A.; et al. A Revised Protocol for Culture of Airway Epithelial Cells as a Diagnostic Tool for Primary Ciliary Dyskinesia. *J. Clin. Med.* **2020**, *9*, 3753. [[CrossRef](#)]
325. Hirst, R.A.; Rutman, A.; Williams, G.; O'Callaghan, C. Ciliated Air-Liquid Cultures as an Aid to Diagnostic Testing of Primary Ciliary Dyskinesia. *Chest* **2010**, *138*, 1441–1447. [[CrossRef](#)] [[PubMed](#)]
326. Schamberger, A.C.; Staab-Weijnitz, C.A.; Mise-Racek, N.; Eickelberg, O. Cigarette smoke alters primary human bronchial epithelial cell differentiation at the air-liquid interface. *Sci. Rep.* **2015**, *5*, 1–9. [[CrossRef](#)] [[PubMed](#)]
327. Pifferi, M.; Montemurro, F.; Cangiotti, A.M.; Ragazzo, V.; Di Cicco, M.; Vinci, B.; Vozzi, G.; Macchia, P.; Boner, A.L. Simplified cell culture method for the diagnosis of atypical primary ciliary dyskinesia. *Thorax* **2009**, *64*, 1077–1081. [[CrossRef](#)] [[PubMed](#)]
328. Neugebauer, P.; Endepols, H.; Mickenhagen, A.; Walger, M. Ciliogenesis in submersion and suspension cultures of human nasal epithelial cells. *Eur. Arch. Oto-Rhino-Laryngology* **2003**, *260*, 325–330. [[CrossRef](#)]
329. Marthin, J.K.; Stevens, E.M.; Larsen, L.A.; Christensen, S.T.; Nielsen, K.G. Patient-specific three-dimensional explant spheroids derived from human nasal airway epithelium: A simple methodological approach for ex vivo studies of primary ciliary dyskinesia. *Cilia* **2017**, *6*, 3. [[CrossRef](#)]
330. de Jong, P.M.; van Sterkenburg, M.A.; Hesseling, S.C.; Kempenaar, J.A.; Mulder, A.A.; Mommaas, A.M.; Dijkman, J.H.; Ponec, M. Ciliogenesis in human bronchial epithelial cells cultured at the air-liquid interface. *Am. J. Respir. Cell Mol. Biol.* **1994**, *10*, 271–277. [[CrossRef](#)]
331. Cao, X.; Coyle, J.P.; Xiong, R.; Wang, Y.; Heflich, R.H.; Ren, B.; Gwinn, W.M.; Hayden, P.; Rojanasakul, L. Invited review: Human air-liquid-interface organotypic airway tissue models derived from primary tracheobronchial epithelial cells—Overview and perspectives. *Vitr. Cell. Dev. Biol.-Anim.* **2021**, *57*, 104–132. [[CrossRef](#)]
332. Horani, A.; Brody, S.L.; Ferkol, T.W.; Shoseyov, D.; Wasserman, M.G.; Ta-shma, A.; Wilson, K.S.; Bayly, P.V.; Amirav, I.; Cohen-Cymberknob, M.; et al. CCDC65 Mutation Causes Primary Ciliary Dyskinesia with Normal Ultrastructure and Hyperkinetic Cilia. *PLoS ONE* **2013**, *8*, e72299. [[CrossRef](#)]

333. Loges, N.T.; Antony, D.; Maver, A.; Deardorff, M.A.; Güleç, E.Y.; Gezdirici, A.; Nöthe-Menchen, T.; Höben, I.M.; Jelten, L.; Frank, D.; et al. Recessive DNAH9 Loss-of-Function Mutations Cause Laterality Defects and Subtle Respiratory Ciliary-Beating Defects. *Am. J. Hum. Genet.* **2018**, *103*, 995–1008. [[CrossRef](#)]
334. Munye, M.M.; Shoemark, A.; Hirst, R.A.; Delhove, J.M.; Sharp, T.V.; McKay, T.R.; O’Callaghan, C.; Baines, D.L.; Howe, S.J.; Hart, S.L. BMI-1 extends proliferative potential of human bronchial epithelial cells while retaining their mucociliary differentiation capacity. *Am. J. Physiol. Cell Mol. Physiol.* **2017**, *312*, L258–L267. [[CrossRef](#)]
335. Cindrić, S.; Dougherty, G.W.; Olbrich, H.; Hjejlić, R.; Loges, N.T.; Amirav, I.; Philipsen, M.C.; Marthin, J.K.; Nielsen, K.G.; Sutharsan, S.; et al. SPEF2- and HYDIN -Mutant Cilia Lack the Central Pair-associated Protein SPEF2, Aiding Primary Ciliary Dyskinesia Diagnostics. *Am. J. Respir. Cell Mol. Biol.* **2020**, *62*, 382–396. [[CrossRef](#)] [[PubMed](#)]
336. Wallmeier, J.; Frank, D.; Shoemark, A.; Nöthe-Menchen, T.; Cindrić, S.; Olbrich, H.; Loges, N.T.; Aprea, I.; Dougherty, G.W.; Pennekamp, P.; et al. De Novo Mutations in FOXJ1 Result in a Motile Ciliopathy with Hydrocephalus and Randomization of Left/Right Body Asymmetry. *Am. J. Hum. Genet.* **2019**, *105*, 1030–1039. [[CrossRef](#)]
337. Hockemeyer, D.; Jaenisch, R. Induced Pluripotent Stem Cells Meet Genome Editing. *Cell Stem Cell* **2016**, *18*, 573–586. [[CrossRef](#)] [[PubMed](#)]
338. Firth, A.L.; Dargitz, C.T.; Qualls, S.J.; Menon, T.; Wright, R.; Singer, O.; Gage, F.H.; Khanna, A.; Verma, I.M. Generation of multiciliated cells in functional airway epithelia from human induced pluripotent stem cells. *Proc. Natl. Acad. Sci. USA* **2014**, *111*. [[CrossRef](#)] [[PubMed](#)]
339. Ahmed, E.; Sansac, C.; Fieldes, M.; Bergougnoux, A.; Bourguignon, C.; Mianné, J.; Arnould, C.; Vachier, I.; Assou, S.; Bourdin, A.; et al. Generation of the induced pluripotent stem cell line UHOMi001-A from a patient with mutations in CCDC40 gene causing Primary Ciliary Dyskinesia (PCD). *Stem Cell Res.* **2018**, *33*, 15–19. [[CrossRef](#)]
340. Drick, N.; Dahlmann, J.; Sahabian, A.; Haase, A.; Göhring, G.; Lachmann, N.; Ringshausen, F.C.; Welte, T.; Martin, U.; Olmer, R. Generation of two human induced pluripotent stem cell lines (MHHi017-A, MHHi017-B) from a patient with primary ciliary dyskinesia carrying a homozygous mutation (c.7915C > T [p.Arg2639\*]) in the DNAH5 gene. *Stem Cell Res.* **2020**, *46*, 101848. [[CrossRef](#)] [[PubMed](#)]
341. Sahabian, A.; von Schlehdorn, L.; Drick, N.; Pink, I.; Dahlmann, J.; Haase, A.; Göhring, G.; Welte, T.; Martin, U.; Ringshausen, F.C.; et al. Generation of two hiPSC clones (MHHi019-A, MHHi019-B) from a primary ciliary dyskinesia patient carrying a homozygous deletion in the NME5 gene (c.415delA (p.Ile139Tyrfs\*8)). *Stem Cell Res.* **2020**, *48*, 101988. [[CrossRef](#)]
342. Xu, X.; Dong, L.; Ma, C.; Xu, X.; Wu, H.; Wang, J.; Zhou, P.; Cao, Y.; Wei, Z. Establishment of an induced pluripotent stem cell line from a patient with primary ciliary dyskinesia carrying biallelic mutations in CCNO. *Stem Cell Res.* **2021**, *53*, 102372. [[CrossRef](#)]
343. Dahlmann, J.; Sahabian, A.; Drick, N.; Haase, A.; Göhring, G.; Lachmann, N.; Ringshausen, F.C.; Welte, T.; Martin, U.; Olmer, R. Generation of two hiPSC lines (MHHi016-A, MHHi016-B) from a primary ciliary dyskinesia patient carrying a homozygous 5 bp duplication (c.248\_252dup (p.Gly85Cysfs\*11)) in exon 1 of the CCNO gene. *Stem Cell Res.* **2020**, *46*, 101850. [[CrossRef](#)]
344. Suzuki, S.; Hawkins, F.J.; Barillà, C.; Beermann, M.L.; Kotton, D.N.; Davis, B.R. Differentiation of human pluripotent stem cells into functional airway basal stem cells. *STAR Protoc.* **2021**, *2*, 100683. [[CrossRef](#)]
345. Hawkins, F.J.; Suzuki, S.; Beermann, M.L.; Barillà, C.; Wang, R.; Villacorta-Martin, C.; Berical, A.; Jean, J.C.; Le Suer, J.; Matte, T.; et al. Derivation of Airway Basal Stem Cells from Human Pluripotent Stem Cells. *Cell Stem Cell* **2021**, *28*, 79–95.e8. [[CrossRef](#)] [[PubMed](#)]